Regulation of Human Neutrophil Responses to *Candida albicans* by Carcinoembryonic Antigen-Related Cell Adhesion Molecule 1 (CEACAM1), CEACAM3 and CEACAM6

Esther Klaile[1], Juan Pablo Prada Salcedo[2], Tilman E. Klassert[1], Matthias Besemer[1], Anne-Katrin Bothe[1], Adrian Durotin[1], Mario M. Müller[1], Verena Schmitt[4], Christian H. Luther[2], Marcus Dittrich[2,3], Bernhard B. Singer[4], Thomas Dandekar[2], Hortense Slevogt[1]

[1]ZIK Septomics, University Hospital Jena, Jena, Germany
[2]Dept. of Bioinformatics, Biocenter, Am Hubland, University of Würzburg, 97074 Würzburg, Germany
[3]Dept. of human genetics, Biocenter, Am Hubland, University of Würzburg, 97074 Würzburg, Germany
[4]Institute of Anatomy, University Hospital, University Duisburg-Essen, Essen, Germany

Running Head: CEACAM6 regulates neutrophil responses to C. albicans

#Address correspondence to: esther.klaile@med.uni-jena.de
Esther Klaile and Juan Pablo Prada Salcedo contributed equally to this work. Author order was determined on the basis of seniority.
Thomas Dandekar and Hortense Slevogt contributed equally to this work. Author order was determined on the basis of alphabetical order.

Abstract

Invasive candidiasis, mainly caused by the pathogen *Candida albicans*, is an important health-care-associated fungal infection that results in mortality rates as high as 40%. Neutrophils are the first line of defense during *Candida* infections. They can launch various killing mechanisms and release cytokines to attract further immune cells to the site of infection. These responses are closely controlled, since they can also result in severe tissue/organ damage. We hypothesized that the regulation of *C. albicans*-specific neutrophil functions by the immunoregulatory *C. albicans* receptors CEACAM1, CEACAM3, and CEACAM6 are involved in the immune pathology of candidemia. Here, we analyzed the effects of specific antibodies targeting the three CEACAM receptors on *C. albicans*-induced neutrophil responses. We show that CEACAM6 ligation significantly enhanced the immediate response to *C. albicans*, as shown by the increased CXCL8/IL-8 degranulation. By assessing the transcriptional responses, we found that CEACAM6 ligation and to some extent CEACAM1 ligation, but not CEACAM3 ligation led to an altered gene regulation of the *C. albicans*-stimulated neutrophils. Differentially expressed genes were analyzed with different bioinformatic methods for the affected cellular processes and signaling pathways including dynamic simulations of signaling cascades. We verified predicted alterations with regard to IL-1β/IL-6 expression and apoptosis induction after *C. albicans* stimulation. Taken together, we could demonstrate for the first time that CEACAM receptors have an important and differential impact in regulating *C. albicans*-induced immune functions in human neutrophils. In particular, CEACAM6 ligation modulated neutrophil apoptosis and cytokine release in responses to *C. albicans*.

Importance

Candida albicans is a major threat to immunosuppressed or critically ill patients. Invasive candidiasis results in mortality rates as high as 40%, even when patients receive antifungal therapy. Neutrophils are key players in the innate host defense against *C. albicans*. They can launch various killing mechanisms, but they also release cytokines to attract further immune cells to the site of infection. However, prolonged attraction of neutrophils is a known risk factor for the development of tissue/organ damage. Here, we analyze how three immunoregulatory receptors of the CEACAM family regulate the neutrophil responses to the major human fungal pathogen, *Candida albicans*. Our data suggest that the inhibition of the CEACAM receptors might be a future therapeutical approach to prevent the overreaction of the immune system such as in systemic infections that often results in organ failure and death of the patients.

Introduction

Invasive candidiasis is the most common fungal disease among hospitalized patients in the developed world, and the fourth most common bloodstream infection in intensive care units (1). Invasive candidiasis results in mortality rates as high as 40%, even when patients receive antifungal therapy, and *Candida albicans* causes the majority of these infections (1).

Neutrophils are key players in the host defense against fungal pathogens. These short-lived innate immune cells react instantly and launch intracellular and extracellular killing mechanisms like the production of reactive oxygen species and microbicidal peptides, or the release of neutrophil extracellular traps (2). Neutrophils also release stored cytokines and produce new ones to attract further immune cells to the site of infection (3). While the total amounts of the secreted cytokines per neutrophil are rather small compared to other immune cells, neutrophils usually greatly outnumber mononuclear leukocytes in inflammatory sites by 1-2 orders of magnitude, implying that they can certainly have a major influence on the local and systemic overall development of the immune response (3).

The neutrophil responses necessary for the quick eradication of pathogens are tightly controlled, since they can also have cytotoxic side effects and result in severe tissue/organ damage, that can subsequently lead to organ failure(s) and the death of the patient (2, 4, 5). Mechanisms for restricted neutrophil activity include the up or down regulation of various surface receptors and intracellular proteins within important signaling pathways, as recently reviewed comprehensively (6). Carcinoembryonic antigen-related cell adhesion molecules (CEACAMs) are immuno-regulatory surface receptors that are able to modulate the activity of a number of important immune receptors, including pattern recognition receptors Toll-like receptor 2 (TLR2) and TLR4 (7-11).

Three members of the CEACAM receptor family that recognize *C. albicans* surface structures are co-expressed on human neutrophils: CEACAM1, CEACAM3, and CEACAM6 (12, 13). The neutrophil marker CEACAM8 (CD66b) does not bind to *C. albicans* (12). While the extracellular domains of CEACAM receptors are composed of highly conserved Ig-like domains, their signaling properties differ widely (11, 14) and can be activating or inhibitory. CEACAM1 is also expressed on various other leukocytes and epithelial cell types (11, 15). The cytoplasmic domain of CEACAM1 bears an immunoreceptor tyrosine-based inhibition motif (ITIM) and recruits Src family kinases and SHP1 and SHP2 phosphatases. Importantly, it can act as both, an activating or an inhibiting receptor (8, 10, 12, 16-19) and delays apoptosis in granulocytes and

lymphocytes (20-22). CEACAM3 is exclusively found on granulocytes and acts as an activating receptor via sign its immunoreceptor tyrosine-based activation motif (ITAM) upon ligation by bacterial pathogens (23, 24). CEACAM6 is GPI-anchored and constitutively localized to membrane microdomains (14). The modulatory roles of CEACAM1, CEACAM3, and CEACAM6 in cellular responses to bacterial pathogens were recently analyzed in detail (8, 25-32). In particular, a comprehensive study on the CEACAM-specific neutrophil responses to *Neisseria gonorrhoeae* in humanized murine neutrophil cell models shows that CEACAM3 mainly mediates neutrophil activation and bacterial killing, while CEACAM1 and CEACAM6 mostly mediate pathogen binding and phagocytosis (28). Interestingly, this study also demonstrates that the co-expression of CEACAM1 and CEACAM6 potentiate, rather than hinder, CEACAM3-dependent responses of neutrophils to the bacterial pathogen (28). Similar results were obtained for *Helicobacter pylori* in murine neutrophils from humanized transgenic mice, where human CEACAM1 expression was sufficient for the binding and the phagocytosis of this pathogen, but an increased ROS production and an enhanced CCL3 secretion was only found in human CEACAM3/CEACAM6-expressing neutrophils, independent of the additional presence of human CEACAM1 (31). However, other studies using neutrophils from Ceacam1$^{-/-}$ mice describe CEACAM1 as an important inhibitory receptor that negatively controls granulopoiesis as well as the LPS-induced IL-1β and ROS production in neutrophils (10, 33). The same mice were used in a study demonstrating the CEACAM1-mediated negative regulation of MMP9 release by mouse neutrophils (12). Also, in mouse monocytes the secretion of IL-6 in response to LPS is regulated by CEACAM1 (34). In human monocytes, CEACAM1 ligation by a peptide mimicking bacterial pathogen binding affects the differentiation into a more pro-inflammatory phenotype resulting in the secretion of high levels of interleukin-1 receptor antagonist and CXCL8 (35).

In the present study, we used CEACAM mono-specific monoclonal antibodies to ligate CEACAM1, CEACAM3 and CEACAM6, respectively, on human neutrophils to analyze their effects on *C. albicans*-induced responses. Recent studies that used different monoclonal antibodies against CEACAM receptors in the absence of pathogens demonstrate that the ligation of either CEACAM on neutrophils resulted in signaling events, priming, and also an enhanced β2-integrin-dependent adhesion to endothelial cells (36, 37). We assessed in the present study, whether neutrophil treatment with various CEACAM-specific antibodies alters different aspects of the immediate response (30-120 min) of human neutrophils to *C. albicans*, including CXCL8 degranulation, ROS production, and transcriptional responses. Moreover, systems biological analysis of the neutrophil transcriptional responses to the CEACAM-specific antibodies in presence or absence of *C. albicans* revealed affected cellular functions that were verified for their long-term (4-24 h) biological effects *in vitro*, like apoptosis and the *de novo* production of IL-6 and IL-1β.

Results:

Increased *C. albicans*-induced CXCL8 release by neutrophil pretreatment with anti-CEACAM6 antibody. In order to establish an easy read-out for the activation of human neutrophils by *C. albicans*, we first ascertained that this stimulation resulted in the early degranulation of CXCL8 (also known as IL-8; Fig 1A). Indeed, stimulation with this fungal pathogen resulted in the rapid secretion of approximately 600 pg CXCL8/ml within 2h (10^7

neutrophils/ml). Pretreatment with the mouse IgG1 isotype control antibody MOPC-21 did not alter CXCL8 release in response to *C. albicans* (Fig. 1A). We then used different mouse monoclonal IgG1 antibodies either monospecific for CEACAM1, CEACAM3, and CEACAM6, or cross-reactive to more than one CEACAM receptor (as indicated in Fig. 1B) for neutrophil ligation before *C. albicans* stimulation. Treatment with the CEACAM6-specific monoclonal antibody 1H7-4B resulted in a strong and significant increase in CXCL8 release upon stimulation with *C. albicans*. One CEACAM1-specific antibody (B3-17) also displayed a considerable increase of CXCL8 release in presence of *C. albicans*, but results from B3-17 treatments did not reach statistical significance due to the high donor-specific variance for the CXCL8 responses. CEACAM6 ligation with 13H10 antibody increased CXCL8 secretion slightly but not statistically significant, while a recombinant CEACAM6-Fc protein did not show any effect on CXCL8 secretion. CEACAM3 ligation with monospecific 308/3-3 did not significantly alter the CXCL8 response to *C. albicans* stimulation, while a slight but not significant increase was detected when monoclonal antibody 18/20 was used that also binds to CEACAM1.

Figure 1C highlights the CXCL8 responses in neutrophil cell culture supernatants from the same donors treated with isotype, B3-17, or 1H7-4B from Figure 1B, respectively. Here, differentially treated samples from the same donor are connected by lines. As depicted, B3-17 treatment always resulted in a small increase of the CXCL8 release compared to the isotype treatment, and 1H7-4B treatment resulted in a strong increase (up to 10-fold) of CXCL8 release, illustrating the donor-independent relative effect of the different antibodies. In absence of *C. albicans* stimulation, no significant CXCL8 secretion or major differences after any antibody treatment were found (Fig. 1D). However, the three most effective antibodies in the presence of *C. albicans* (B3-17, 1H7-4B and 13H10) also resulted in a minor increase (2-fold) of CXCL8 secretion in some neutrophil preparations when used alone in the absence of *C. albicans*. The differences in CXCL8 concentrations between antibody treatment without *C. albicans* stimulation (30-170 pg/ml), and antibody treatment with *C. albicans* stimulation (400-11,000 pg/ml) ranged between one and two orders of magnitude, depending on the donor. The high variation in the release of CXCL8 and other cytokines by neutrophils from different donors are also found in other studies using different stimuli, including the CD11b/CD18 ligand Thy-1, LPS, and fMLP, and many studies therefore give the standard error instead of the standard deviation (38-41). For the following experiments, the CEACAM1-specific antibody B3-17 ("CC1"), the CEACAM3-specific antibody 308/3-3 ("CC3"), and the CEACAM6-specific antibody 1H7-4B ("CC6") were chosen for further investigation.

No influence of anti-CEACAM antibodies on neutrophil-mediated killing of *C. albicans*. We next analyzed the influence of the three CEACAM1/3/6-targeting antibodies on different cellular functions elicited directly upon the engagement of the neutrophil by the fungal pathogen. First, we tested if the antibodies affected *C. albicans* binding to neutrophil cell surfaces (Fig. 2A). In accordance with our findings that the CEACAM family receptors are not critical for *C. albicans* adhesion to different epithelial cell lines (12) and CEACAM1-transgenic mouse neutrophils (42), neutrophil binding to fungal cells was not affected by antibody-mediated CEACAM ligation in two different donors (Fig. 2A). A major killing mechanism employed by neutrophils is the oxidative burst. We therefore tested the production of reactive oxygen species (ROS) under the different antibody treatments in the presence or absence of *C. albicans* stimulation

(Fig. 2B). While ROS production by *C. albicans* stimulation was clearly detected in two different donors, none of the three antibodies used for ligation changed the basic ROS levels in absence of *C. albicans* nor the *C. albicans*-induced ROS levels after infection (Fig. 2B). To test for effects of the antibody treatments on the overall efficiency of fungal killing by the neutrophils, we next analyzed the number of surviving fungal cells after 30 min co-incubation with the neutrophils. None of the tested CEACAM1-, CEACAM3- or CEACAM6-specific monoclonal antibodies showed a detectable effect on neutrophil killing efficiency (Fig. 2C).

The *C. albicans*-induced transcriptional response in neutrophils is differentially enhanced by the ligation of CEACAM1/3/6-directed antibodies. CEACAM receptor ligation by various antibodies results in neutrophil priming and enhanced binding to endothelial cells (36, 37). Therefore, we next examined if antibody-mediated CEACAM ligation on neutrophil surfaces with B3-17 ("CC1"), 308/3-3 ("CC3"), and 1H7-4B ("CC6") would also affect neutrophil transcriptional responses in the presence or absence of *C. albicans* stimulation. Indeed, CEACAM ligation with the monospecific antibodies in the presence and in the absence of *C. albicans* stimulation affected transcriptional responses. Principal component analyses (PCA, Figs. 3A, S1A) demonstrated that the different antibody treatments in the presence or the absence of *C. albicans* stimulation were well separated and that the data had a good quality. Principal component analysis (PCA, Fig. 3A) revealed that CC6 treatment had the largest influence on the neutrophil transcriptomic response induced by *C. albicans*, followed by CC1 treatment. CC3 treatment before *C. albicans* infection only resulted in minor alterations in gene transcription. The three antibodies displayed similar hierarchies in absence of *C. albicans* stimulation (Fig S1A).

We first analyzed the transcriptional response induced by *C. albicans* stimulation. IgG treatment with subsequent *C. albicans* stimulation of neutrophils resulted in 436 significantly differentially expressed genes (DEGs) compared to IgG treatment in absence of *C. albicans* stimulation: 207 DEGs were up-regulated and 229 were down-regulated (fold-change >±2, adjusted p-value <0.05; see Table S1 for details). We then investigated significant differences in the gene expression after *C. albicans* stimulation induced by the pre-treatment with the different anti-CEACAM antibodies, respectively. Anti-CEACAM1 treatment in presence of *C. albicans* stimulation resulted in 37 DEGs compared to IgG treatment in presence of *C. albicans* stimulation, with 36 upregulated genes and 1 downregulated gene (Table S1). Anti-CEACAM6/*C. albicans* treatment caused 122 DEGs compared to IgG/*C. albicans* treatment, with 105 upregulated and 17 downregulated genes (Table S1). Systems biology analysis showed that 39 of the upregulated genes were synergistically co-regulated by *C. albicans*. In contrast, anti-CEACAM3/*C. albicans* treatment led to the differential expression of only 4 genes compared to the IgG/*C. albicans* treatment (Table S1). Figure 3B displays the comparison of the DEGs induced by the three CEACAM-specific antibodies with *C. albicans* stimulation, respectively. All DEGs used for the calculation of Fig. 3B and their affiliation with the respective partitions of the Venn diagram are listed in Table S3. The four genes increased by anti-CEACAM3/*C. albicans* treatment were also upregulated by anti-CEACAM1/*C. albicans* and anti-CEACAM6/*C. albicans* treatment. Anti-CEACAM1/*C. albicans* treatment also shared the majority of regulated genes with anti-CEACAM6/*C. albicans* treatment (26 of 37 DEGs). 92 of the DEGs induced by anti-CEACAM6/*C. albicans* treatment were unique to this treatment.

We then compared DEGs induced by CEACAM1 ligation with the B3-17 antibody in presence of *C. albicans* stimulation (Table S1) with the effect of the CEACAM1 antibody alone (without *C. albicans* stimulation, Table S2). DEGs not shared by both groups (Fig 3 C, Table S4) were analyzed for significantly enriched Gene Ontology (GO) categories. Please note that only protein-coding genes are annotated in the GO database. Differences between to the numbers given in Figures 3C (and 3D, see below) are due to non-protein coding transcripts that were included in the Venn diagram. Within the 15 protein-coding DEGs only found in the treatment by anti-CEACAM1 antibody alone (Fig. 3C, CC1), no GO category was significantly enriched. Of the 16 protein-coding DEGs only found in the anti-CEACAM1 antibody treatment with *C. albicans* stimulation (Fig. 3C, CC1+Ca), seven were annotated to be involved in the significantly enriched GO category "positive regulation of protein phosphorylation". A similar comparison of anti-CEACAM6 antibody treatment in absence and presence of *C. albicans* stimulation (Fig. 3D, Table S5) revealed the following significantly enriched GO categories. Within the 60 protein-coding DEGs induced by anti-CEACAM6 antibody alone, 12 were annotated to be involved in "leukocyte activation", 14 were annotated to the "cellular response to cytokine stimulus", and 17 to the "regulation of immune system process". Of the 34 protein-coding DEGs only induced by anti-CEACAM6 antibody with subsequent *C. albicans* stimulation, four were annotated to the "the regulation of TLR-responses", four to "ROS metabolic processes" and 13 to the "positive regulation of gene expression". These data suggest that CEACAM1 ligation and in particular CEACAM6 ligation are likely able to influence important long-term neutrophil functions in response to *C. albicans*.

A comparison of the genes induced by the respective anti-CEACAM antibodies alone (without *C. albicans* stimulation, Fig. 3E, Table S6) revealed that anti-CEACAM3 treatment shared four of its five upregulated genes with both, anti-CEACAM1 and anti-CEACAM6 treatments, and the fifth gene only with anti-CEACAM1 treatment. Also, anti-CEACAM1 antibody treatment shared the majority of DEGs with anti-CEACAM6 antibody treatment (29) and displayed only 5 unique DEGs. Anti-CEACAM6 antibody treatment resulted in 117 unique DEGs (Fig. 3E, Table S6).

GO enrichment analysis of all differentially regulated genes by anti-CEACAM6 antibody treatment in presence of *C. albicans* (Table S1) revealed that many are implicated in the regulation of major neutrophil functions. Selected functions are represented in the heatmaps shown in Fig. 4, highlighting the differences in transcriptomic responses elicited by the different CEACAM ligating antibodies. Significantly enriched GO categories after CEACAM6/ *C. albicans* treatment included cell adhesion/migration, cytokine production, secretion, and the cellular responses to cytokines. Importantly, also genes of proteins annotated to programmed cell death were enriched after CEACAM6 ligation and *C. albicans* stimulation (Fig. 4). A similar analysis of DEGs induced by anti-CEACAM1 antibody treatment in presence of *C. albicans* (Fig. S1B) revealed the enrichment of some, but not all cellular functions found enriched after anti-CEACAM6/*C. albicans* treatment. This was expected from the partial overlap between the DEGs found in both treatments (Fig. 3B). Apoptosis was not among the enriched functions.

Integrated network analysis and dynamic models predict the modulation of *C. albicans*-induced apoptosis by anti-CEACAM6 antibody treatment. The gene expression data sets further allowed a systems biological analysis of the signaling events involved. Since anti-

CEACAM6 treatment had the most profound influence on the neutrophil transcriptional response in the presence of *C. albicans* stimulation, we further analyzed the cellular functions affected in dynamic models, and signaling pathways likely leading to these alterations in the cellular functions (Figs. 5, 6). We considered signaling cascades triggered from the CEACAM6 ligation via direct protein-protein interactions as well as downstream pathways and functions induced subsequentially according to the CEACAM6-specific transcriptional response (detailed procedures are given in the Methods section).

Thus, for CEACAM6 treatment in the presence of *C. albicans* stimulation, the integrated network analysis identified an optimally responsive network module of 136 genes with 174 interactions (Fig. 5). The network module comprised many key players in apoptosis and NF-kappa B (NFκB) signaling, also reflected by the highly significant enrichment of KEGG pathways related to these and other functions (Fig. 5, Table S7). The KEGG pathways overlapped to some degree, since many signaling molecules are shared by different pathways. Central to the regulation of apoptosis and cytokine production are molecules of the NFκB complex and associated signaling partners, as illustrated in Fig. 5, displaying the overlapping pathways. Interestingly, also the regulation of TLR signaling was significantly enriched by CEACAM6 treatment (Table S7). So far, only for CEACAM1 and CEACAM3 experimental evidence is available for the regulation of these important pattern recognition receptors (8-10, 24, 43), which can recognize both, bacterial and fungal pathogens (44).

Dynamical network analysis of transcriptional data from the CEACAM6-treated neutrophils in the presence of *C. albicans* distinguished key players annotated to cellular functions according to the Gene Ontology (GO) data base that were induced by the CEACAM6 ligation (Fig. 6). The cell function-centered network analysis verified that both, the regulation of cytokine production and the regulation of apoptosis were among the most significantly enriched cellular functions (Fig. 6, Table S8). Also, the regulation of cytokine production, cell migration, and other basic functions important for the execution of neutrophil responses, including the regulation of TLR signaling, were strongly enriched (Fig. 6, Table S8). Moreover, dynamical simulations based on the transcriptomic data predicted the activation of caspase-8 (CASP8) and CASP1, two molecules recognized as central switches for apoptosis (45, 46), by anti-CEACAM6 treatment in presence of *C. albicans* stimulation, but not by CEACAM1/*C. albicans* treatment (Fig. S2). The same dynamical simulations also predict an undulating behavior of the *IL6* response with a delayed activity from the first impulse given by the pathogen stimulus. Thus, the predictions by the cell function-centered network analysis are in agreement with the projections of the pathway-centered integrated network analysis.

Verification of the biological significance of predicted alterations of neutrophil functions. Taken together, the different bioinformatic approaches identified programmed cell death/apoptosis as one of the cellular functions most dominantly affected by CEACAM6 treatment in presence of *C. albicans* stimulation (DEGs are listed in Table S1; details for bioinformatics are given in the Methods section). None of the other antibody treatments either in the presence or in the absence of stimulation by *C. albicans* resulted in the enrichment of this feature, indicating a specificity for CEACAM6 to regulate *C. albicans*-induced apoptosis. In contrast, the induction of the production of several cytokines was modulated by antibody treatment against the three CEACAM receptors alone, as well as in presence of *C. albicans*

stimulation (Tables S1, S2). Also, the bioinformatic approaches predicted cytokine production and associated pathways to be modulated after CEACAM1 and CEACAM6 treatment (Figs. 5, 6, S1C, Tables S7, S8,). We therefore analyzed the neutrophil apoptosis and the production of the pro-inflammatory cytokine interleukin-1β (IL-1β) in detail in long-term experiments.

As just mentioned, the significant enrichment of DEGs with gene products annotated to be linked to the regulation and execution of programmed cell death was only found by GO enrichment analysis, pathway network analysis (Fig 4) and functional network analysis (Fig.5) for anti-CEACAM6 treatment in presence of *C. albicans* stimulation. *In vitro* experiments with CEACAM ligation and *C. albicans* stimulation completely supported these predictions (Fig. 7). CEACAM6 ligation with the monoclonal antibody 1H7-4B was enhanced the *C. albicans*-induced apoptosis of human neutrophils, while none of the antibody treatments targeting CEACAM1 or CEACAM3 altered the neutrophil apoptosis (Fig. 7A, B). Moreover, neither the anti-CEACAM6 antibody nor the anti-CEACAM1 and anti-CEACAM3 antibodies affected the spontaneous apoptosis (without *C. albicans* stimulation) of the neutrophils after 4 h and after 24 h, respectively (Fig. 7C, D).

For the predicted cytokine production, a more complex situation presented itself in the bioinformatic analyses as well as by a simple look at the transcriptional data. Network analyses and GO enrichment predicted a general NFκB-dependent enhancing influence of both, CEACAM1 and CEACAM6, on the production of cytokines and on the cellular response to the cytokines (Figs. 3, 4, 5). Both effects can influence the sensor and effector functions of the neutrophils, putatively altering the long-term cytokine *de novo* synthesis and release. We chose the important pro-inflammatory cytokine IL-1β for the verification of the prediction model derived from the transcriptomic data set.

Transcription of the *IL1B* gene was only moderately induced by *C. albicans* stimulation of human neutrophils at 2 h and also moderately enhanced by CEACAM1 treatment with and without *C. albicans* stimulation (Fig.8A). CEACAM3 treatment had no significant impact on the *IL1B* gene expression at 2 h, while CEACAM6 treatment enhanced the *IL1B* expression in the presence and the absence of *C. albicans* (Fig.8A). When we analyzed the secretion of IL-1β protein into the cell culture supernatants after 21 h (Fig. 8B, C), we found that *C. albicans* stimulation indeed increased the total release of IL-1β from 5.7 ±1.5 pg/ml ("Untreated", Fig. 8B) to 40.0 ±12.4 pg/ml ("Untreated +*C. albicans*", Fig 8C). However, in contrast to the CEACAM1 treatment-evoked increase in the *IL1B* transcripts, it did not result in detectable differences compared to isotype-treated neutrophils neither in the presence nor absence of *C. albicans* stimulation (Fig. 8B, C). Interestingly, CEACAM3 treatment led to a significant increase in IL-1β secretion with or without *C. albicans* stimulation, despite the unaltered *IL1B* transcription levels after 2 h (Fig. 8B, C). Concordant with the transcriptional response, CEACAM6 treatment resulted in a significant increase in IL-1β secretion in the presence of *C. albicans* stimulation at 21 h (Fig. 8C). In the absence of the fungal pathogen IL-1β levels were moderately but not significantly enhanced at 21 h (Fig. 8C).

The CEACAM3 ligation-induced IL-1β production, despite the lack of a detectable increase in the transcriptional activity after 2 h, led us to reinvestigate our network analysis. The sub-network analysis revealed a possible interaction between *IL6* and the subsequent induction of *IL1B* (Fig. 9A). Importantly, the regulation goes both ways, i.e., IL-1β is not only able to induce IL-6, but it can, *vice versa*, also be induced by IL-6. However, in contrast to the well-known "direct"

induction of IL-6 via IL-1β, there were at least 4 nodes between *IL6* and *IL1B* (Fig. 9A). Still, *IL6* was among the few genes upregulated by CEACAM3 treatment (Fig. 9B). *IL6* was actually significantly upregulated by all three anti-CEACAM antibodies in the presence and in the absence of *C. albicans*, respectively, but IL-6 expression was not affected by *C. albicans* alone (Fig. 9B). However, in untreated and isotype-treated neutrophils hardly any *IL6* transcripts were detected by sequencing. The normalized counts of the *IL6* transcripts were between 0 and 3 in the presence and the absence of *C. albicans* stimulation in untreated neutrophils, and also in isotype-treated neutrophils. Normalized counts in all CEACAM treatment groups with or without *C. albicans* stimulation were in the range between 24 and 1447. Thus, very few transcripts serve neutrophils for the *de novo* synthesis of this pro-inflammatory cytokine.

To analyze if these few transcripts are translated into detectable protein levels and secreted after contact with *C. albicans*, we measured IL-6 levels in neutrophil supernatants after 21 h of infection (Fig. 9C, D). The lack of transcriptional *IL6* expression and induction by *C. albicans* was verified *in vitro* via ELISA, where 3.7±1.7 pg/ml IL-6 were produced by untreated neutrophils in the absence, and 4.5±1.2 pg/ml IL-6 in the presence of *C. albicans* (Fig. 9C and D, respectively; 10^7 neutrophils/ml). As predicted, CEACAM3 treatment significantly enhanced the IL-6 secretion in the absence and the presence of *C. albicans*, respectively (Fig. 9C, D). Also, CEACAM6 treatment augmented the IL-6 release with and without *C. albicans* stimulations slightly but significantly (Fig. 9C, D). CEACAM1 treatment only resulted in minor, non-significant increases in IL-6 secretion, both, in presence and in absence of *C. albicans* stimulation (Fig. 9C, D), despite a strong transcriptional induction at 2 h.

Discussion

Here, we show for the first time that CEACAM receptors expressed on human neutrophils influence the human neutrophil response to *C. albicans*. CEACAM6 ligation of human neutrophils in the presence of *C. albicans* stimulation enhanced the early release of CXCL8 and altered the neutrophil transcriptional responses. Different bioinformatic approaches (transcriptome analysis, network analysis and dynamical modelling of the involved response) then led to the identification of long-term neutrophil responses modulated by the CEACAM6-treatment in *C. albicans*-stimulated neutrophils, i.e., *C. albicans*-induced apoptosis and IL-6/IL-1β *de novo* synthesis.

It was surprising to find that the degranulation of CXCL8 and the global transcriptional response after 2 h of *C. albicans*-stimulation were enhanced by the antibody-mediated ligation of CEACAM1 (by B3-17) and CEACAM6 (by 1H7-4B), but not of CEACAM3 (by 308/3-3). On neutrophils, CEACAM3 is recognized as the central CEACAM family receptor leading to neutrophil activation by bacteria, and the subsequent phagocytosis and bacterial killing due to an ITAM in its cytoplasmic tail (23-25, 28, 47-51). Despite the dominance of CEACAM3 in the human neutrophil responses to pathogenic bacteria, both, CEACAM1 and CEACAM6, can also mediate binding and phagocytosis of bacterial pathogens in neutrophils and in other cell types (28, 51, 52). In epithelial cells, CEACAM1 induces either inhibitory or activating effects on their immune responses; e.g., in lung epithelial cells, CEACAM1 dampens TLR2-mediated responses (8, 18), while it is critical for the pathogen-induced CXCL8 release in gastric and intestinal cell lines (12, 17).

In accordance with our findings in epithelial cells (12, 17), CEACAM1 ligation with B3-17 antibody mostly induced activating functions within the immediate neutrophil response to *C. albicans*, e.g., enhancing the CXCL8 degranulation. Interestingly, the long-term response of the neutrophils seemed rather dampened by CEACAM1 ligation, since the two important pro-inflammatory cytokines IL-6 and IL-1β were not enhanced in the CEACAM1 treated neutrophils in the presence and the absence of *C. albicans* stimulation, respectively. It is likely that the CEACAM1 negative regulation on IL-6 and IL-1β secretion takes place at some point after the increased transcription of these two cytokines, since the *IL1B* and the *IL6* gene transcription was significantly upregulated by CC1 treatment. The precursor of IL-1β is biologically inactive and requires proteolytic cleavage into biologically active mature cytokines, controlled by the inflammasome-mediated caspase-1 activation (53). Hence, a two-step model has been proposed for IL-1β production: first, activation of PRRs on host cells induce enhanced synthesis of pro-IL-1β; second, activation of the inflammasome by PAMPs results in the posttranslational cleavage of the pro-cytokine into mature IL-1β (54). It is thus possible for CEACAM1 to influence the transcription of *IL1B* on the one side, and on the other inhibit the release of the active cytokine by inhibition of the subsequent processing steps. In fact, in mouse neutrophils, CEACAM1 negatively regulates the LPS-induced IL-1β production by blocking caspase-1 activation (10). Also the function of another essential receptor on mouse neutrophils, granulocyte-stimulating growth factor receptor, is inhibited by CEACAM1, resulting in a reduced granulopoiesis (33). And on mouse monocytes, CEACAM1 can negatively regulate IL-6 production (34). These dampening effects of CEACAM1 on the mouse myeloid responses enhanced the susceptibility of mice to bacterial pathogens and LPS challenge *in vivo* (33, 34). It should also be noted that not all specific antibodies used in this study evoked the same effects or affected neutrophil functionality to variable magnitude when CEACAM1, CEACAM3 or CEACAM6 were ligated. Different antibodies to CEACAM1 can either enhance or block CEACAM1-mediated adhesion in trans and thereby can modulate the dimerization status of CEACAM1 or intracellular binding of SHP1 and SHP2 phosphatases and Src-like kinases to the CEACAM1-long cytoplasmic domain (55). Furthermore, it is well established that CEACAM1 ligation on epithelial cells can transduce inhibitory or activating cell signaling events dependent on the cellular status or context of the same cell (56). Taken together, our data disclose different roles for CEACAM1 ligation in the immediate neutrophil response to *C. albicans* (enhanced CXCL8 degranulation, altered transcriptional responses), and in the long-term response to *C. albicans* (inhibition of further pro-inflammatory signals in form of IL-1β secretion), the latter being similar to CEACAM1-mediated regulation of neutrophil responses to bacterial pathogens.

CEACAM3 also played a dualistic role in the neutrophil responses to *C. albicans*. While there were no alterations upon CEACAM3 ligation in the immediate neutrophil responses (CXCL8 release, binding, fungal killing), and only four genes were significantly upregulated after 2 h of *C. albicans* stimulation, CC3 treatment resulted in the highest concentrations of IL-1β and IL-6 after 21 h incubation of all treatment groups. Thereby, CEACAM3 ligation showed the highest potential of increasing local inflammation with all its cytotoxic side effects (2, 4). Interestingly, based on the transcriptional responses obtained 2 h post-infection, IL-6 production preceded IL-1β production. Sub-network analysis revealed a potential induction of IL-1β by increased IL-6 levels via several pathways with four or more nodes in between the two cytokines. The majority of these

pathways leading from IL-6 to IL-1β activation included the intermediate step of either CXCL8 or CCL20 production. Taken together, the role of CEACAM3 in the regulation of neutrophil responses to the fungal pathogen studied here and to various bacterial pathogens discussed earlier, differs widely: CEACAM3 has a major activating effect on the immediate response to the bacterial pathogens, but regulates rather long-term events affecting and enhancing the overall inflammatory response in *C. albicans* infection.

Network analysis and systems biological modelling were done here to get a first systems view on succession of events in the CEACAM receptor networks and their connection to apoptosis, inflammation and chemokine production. Integrated network analysis is capable of detecting signals beyond the scope of classical pathway analysis as it integrates the semantic of an interaction network. It is not confined to pre-established (known) pathways but rather includes the entire interaction network and thus has the power to also disentangle complex receptor pathway cross stimulation (57). Subsequent pathway enrichment then allows to functionally characterize the module and can further elucidate the intricate structure of complex pathways. Predictions from the comprehensive bioinformatic approaches used in this study on the unique behavior of CEACAM1, CEACAM3, and CEACAM6 (see discussion below) in *C. albicans*-stimulated neutrophils over time fit well to the *in vitro* data presented.

For CEACAM6 ligation, all three bioinformatic approaches consistently predicted an influence on the *C. albicans*-induced apoptosis. In contrast, no such prediction arose for CEACAM1 ligation. This was rather surprising, since our earlier publication shows that in rat granulocytes, CEACAM1 delays the spontaneous and the FAS ligand-mediated apoptosis (20), while on lung epithelial and colorectal cancer cells, CEACAM1 supports apoptosis (58, 59). In the experimental set-up used here, only CEACAM6 ligation in presence of *Candia*-stimulation lead to an enhanced apoptosis. All other treatments did not alter survival of the neutrophils compared to untreated neutrophils in presence or absence of *C. albicans* stimulation, respectively. So far, most studies show that CEACAM6 mostly decreases apoptosis and anoikis (apoptosis induced by the lack of adhesion) in various cancer cells and in primary epithelial cells (60-66). Interestingly, one study on acute lymphoblastic leukemia also demonstrates an increase in apoptosis via antibody-mediated ligation of CEACAM6 (67).

The CEACAM6-induced *de novo* production of IL-1β and IL-6 also was in accordance with the transcriptional analysis and the bioinformatic predictions. An increase of CEACAM6 expression on epithelial cells and leukocytes is induced by various pathogens and pro-inflammatory cytokines (12, 68-71) and is thus generally associated with inflammatory events. CEACAM6 interaction on ileal mucosa with adherent-invasive *E. coli* (AIEC), bacterial pathogens associated with Crohn disease (CD), results in an enhanced inflammation *in vivo*, both, in CD patients and in a CD mouse model using CEABAC10 transgenic mice (71, 72). Further, CEACAM6-AIEC interaction also enhances cytokine production in mucosal cells *in vitro* (68, 71). On neutrophils, increased CEACAM6 expression levels are correlated with asthma severity (73). The latter study proposes the presence of an altered neutrophil phenotype in presence of increased CEACAM6 expression. To our knowledge, this is the first study showing that CEACAM6 ligation enhances neutrophil cytokine production. Our experiments also likely underestimated the levels of IL-1β and IL-6 produced per neutrophil upon anti-CEACAM6 treatment with the 1H7-4B antibody during

C. albicans infection, since the same treatment also led to an increase in apoptosis, thereby reducing the numbers of neutrophils contributing to the cytokine levels.

However, neutrophils co-express not only CEACAM1, CEACAM3 and CEACAM6, but also CEACAM8 and CEACAM4. Of these, the former three are likely co-stimulated by *C. albicans*. Furthermore CEACAM receptors are able to modulate the functions of other members of the CEACAM family (37). Therefore, further experiments will be necessary to determine the exact roles of the single CEACAM family members during neutrophil responses to *C. albicans*, and whether one CEACAM receptor is dominant in the response to the pathogen. Since neutrophils are short-lived and therefore are not useful for the transfection with siRNA, ligation with antibodies remains the best accessible tool. Any CEACAM-monospecific or even cross-reacting antibody (mimicking co-ligation by the pathogen) has to be evaluated on its own and in the specific setting of the experiment, since targeting different epitopes on the same CEACAM receptor can either enhance or inhibit the receptor functions (55), and one antibody can elicit inhibitory or activating cell signaling events dependent on the cellular condition of the same cell (56). While neutrophils from transgenic mice expressing one or more human CEACAMs proved valuable for the determination of the role of CEACAM receptors in the neutrophil response to bacterial pathogens (28, 31, 48), our data obtained with *C. albicans* stimulated neutrophils from human CEACAM1-transgenic mice suggest that mouse neutrophils do not respond to the fungal pathogen in a CEACAM1-dependent manner. Since mice are inherently naïve for *C. albicans* infection, it is possible that some (co-)receptor or signaling protein important for the CEACAM-specific response to this human pathogen is lacking in the mouse neutrophils.

Taken together, the combination of transcriptome analysis, cytokine measurements and systems biological modelling in the present study revealed that antibody-mediated ligation of CEACAM1, CEACAM3, and CEACAM6 could elicit specific regulations of neutrophil responses, evoked by the fungal pathogen *C. albicans.* CEACAM1 ligation had an early activating effect on human neutrophils during *C. albicans* infection (CXCL8 release, transcriptome), but acted inhibitory on the long-term response (IL-1β secretion). CEACAM3 ligation had only minor early effects during *C. albicans* infection, but acted strongly pro-inflammatory in long-term experiments (IL-6 and IL-1β release). CEACAM6 ligation consistently displayed an activating activity in neutrophils in early (CXCL8 release, transcriptome) and long-term (IL-6 and IL-1β release) responses. Interestingly, CEACAM6 ligation also resulted in an enhanced *C. albicans*-induced apoptosis.

Materials and Methods

Neutrophil isolation and treatments. Human peripheral blood was collected from healthy volunteers with written informed consent. This study was conducted according to the principles expressed in the Declaration of Helsinki. The blood donation protocol and use of blood for this study were approved by the institutional ethics committee of the University Hospital Jena (permission number 5070-02/17). Neutrophils were isolated from peripheral blood using 1-Step Polymorphs (GENTAUR GmbH, Germany). In brief, 20 ml 1-Step Polymorphs were overlaid with 20 ml blood and centrifuged at 500 × g for 35 min at room temperature with acceleration and deceleration set to “0”. The lower cell layer was collected, mixed with one volume of ice-cold

513 0,45% NaCl solution, and centrifuged at 4°C and 400 × g for 10 min. the pellet was suspended in
514 5 ml ice-cold ACK lysis buffer. The reaction was stopped by adding 45 ml HBSS (GIBCO, Thermo
515 Fisher Scientific, Germany). Centrifugation for pelleting and a further washing step using HBSS
516 were performed at 4°C and 250 × g for 10 min. Purity >96% was determined by flow cytometry.
517 Cells numbers were adjusted to 1×10^7 cells/ml in RPMI/10% FBS if not stated otherwise and
518 experiments were performed immediately. Cells were either left untreated or treated with 10 µg/ml
519 antibody (see below) for 45 min. Cells were then either left unstimulated or stimulated with
520 *C. albicans* for 2 h at an MOI of 1 if not mentioned otherwise.
521 **Antibodies and recombinant CEACAM6-Fc.** All antibodies used were monoclonal mouse IgG1:
522 MOPC-21 (Hoelzel Diagnostika GmbH, Germany; isotype control), B3-17 (anti-human
523 CEACAM1, Singer, Essen, Germany), C5-1X/8/8 (anti-human CEACAM1, Singer, Essen,
524 Germany), CC1/3/5-Sab (anti-human CEACAM1/3/5, LeukoCom, Essen, Germany), 18/20 (anti-
525 human CEACAM1/3/5, Singer, Essen, Germany), 308/3-3 (anti-human CEACAM3/5, LeukoCom,
526 Essen, Germany), 1H7-4B (anti-human CEACAM6, LeukoCom, Essen, Germany), 13H10 (anti-
527 human CEACAM6, Genovac, Freiburg, Germany). Specificity of all antibodies was verified by
528 FACS analysis using CHO or HELA cells transfected with human CEACAM1, CEACAM3,
529 CEACAM6, CEACAM5, CEACAM8, or empty vector (negative control). Note that none of the
530 antibodies cross-reacted to CEACAM8, and that 18/20, CC1/3/5-Sab, and 308/3-3 cross-reacted to
531 CEACAM5 that is not expressed on neutrophils (therefore we refer to 308/3-3 as "CEACAM3-
532 specific" in the context of this publication). Cross-reactivities to CEACAM1, CEACAM3, and
533 CEACAM6 are given in Figure 1. Recombinant CEACAM6 protein consisting of the CEACAM6
534 extracellular domain fused to the constant region of human IgG were produced in HEK-293 cells
535 and purified via protein G columns (GE Healthcare, Munich, Germany) as described previously
536 (74).
537 ***Candida albicans***. *C. albicans* strain SC5314 was grown as described (75, 76). For experiments,
538 YPD liquid cultures were inoculated with a single colony from YPD agar plates and grown at 30°C
539 and 180-200 rpm for 14-16 h. Yeast cells were harvested, washed twice and suspended in a desired
540 volume of ice-cold PBS. Yeast cells were counted in a Neubauer Improved chamber.
541 **ELISA** 1×10^7 neutrophils/ml in RPMI/10% FBS were either left untreated or treated with 10 µg/ml
542 antibody for 45 min. Cells were then either left unstimulated or stimulated with *C. albicans* for 2
543 h at an MOI of 1. Supernatants were harvested at the indicated time points and tested for CXCL8
544 (BD Biosciences, Germany; sensitivity: 3 pg/ml), IL-6 (Abcam, Germany; sensitivity: 2 pg/ml)
545 and/or IL-1β (sensitivity: 4 pg/ml) concentrations by ELISA (BD Biosciences, Germany).
546 **Binding analysis and ROS determination** Neutrophils were stained with anti-CD11b-PerCP-
547 Vio700 (REA592, Milteyi Biotech, Germany; 5 µl for 4×10^6 neutrophils in 400 µl medium) for 45
548 min. *C. albicans* cells were stained with Rabbit anti-*C. albicans* IgG (BP1006, Acris Antibodies,
549 5 µl for 6×10^7 *C. albicans* cells in 200 µl medium) for 30 min, followed by Goat anti-Rabbit-
550 AlexaFluor633 (Invitrogen, Sweden; 2 µl in 400 µl medium) for 30 min. 2×10^5 stained neutrophils
551 in 200 µl RPMI/10% FBS were left untreated or treated with 10 µg/ml antibody and incubated for
552 45 min at 37°C, 5% CO_2. Neutrophils were left unstimulated or were stimulated with 1×10^6
553 *C. albicans* cells per well (MOI 5) and samples were incubated for 30 min at 37°C, 5% CO_2. 10 µl
554 of 0.5 µg/ml DHR (Sigma-Aldrich, Germany) working solution in 4% FBS/D-PBS (Gibco/Thermo
555 Fisher Scientific, Germany) was added to each sample to reach a final concentration of 25 ng/ml,

and samples were incubated at 37°C, 5% CO_2 for 10 min. Samples were analyzed in an Attune flow cytometer (Invitrogen/ Thermo Fisher Scientific, Germany; BL1: DHR123/ROS, BL3: CD11b/neutrophils, RL1: C. albicans). For adjustments and compensation, separate single staining of samples for all channels was performed before the experiments. Relative fluorescence units of the DHR123/ROS signals were logarithmized for presentation.

Killing assay. In a 96 well plate, 2×10^5 neutrophils in 100 µl RPMI/10% FBS were left untreated or treated with 10 µg/ml antibody in duplicates and incubated for 45 min at 37°C, 5% CO_2. Neutrophils were left unstimulated or were stimulated with 2×10^5 *C. albicans* cells per well (MOI 1) and samples were incubated for 30 min at 37°C, 5% CO_2. *C. albicans* solution for standards (input) was kept on ice for the incubation times. Just before the following procedures, *C. albicans* standards (sensitivity: 6,500 CFU) were transferred to the 96 well plate. Triton X-100 was added to all wells to reach a final concentration of 0,3% and incubated for 10 min at 37°C, 5% CO_2, in order inactivate neutrophils. Viable *C. albicans* cells were quantified using the Colorimetric Cell Viability Kits III (XTT) from Promokine, Germany: 50 µl XTT reaction mixture was added per well and samples were incubated for further 3-4 h at 37°C, 5% CO_2. Absorbance was measured using a TECAN M200 at 450 nm and 630 nm (background). For calculations of *C. albicans* CFUs, background and blanks were subtracted.

Spontaneous and *C. albicans*-induced apoptosis. 2×10^5 neutrophils in 200 µl RPMI/10% FBS were left untreated or treated with 10 µg/ml antibody in duplicates and incubated for 2 h at 37°C, 5% CO2. Neutrophils were left unstimulated (spontaneous apoptosis) or were stimulated with 2×10^5 C. albicans cells per well (MOI 1; C. albicans-induced apoptosis) and samples were incubated for 4 h or 24 h (unstimulated only) at 37°C, 5% CO2. Cells were stained with the Annexin V Detection Kit APC (eBioscience, Germany) and analyzed in an Attune flow cytometer (Invitrogen/ Thermo Fisher Scientific, Germany; BL2: propidium iodide, RL1: Annexin V-APC). Cells negative for PI and Annexin V were considered viable.

RNA sequencing. 1.2×10^7 neutrophils in 1.2 ml in RPMI/10% FBS were either left untreated or treated with 10 µg/ml antibody for 45 min. Cells were then either left unstimulated or stimulated with *C. albicans* for 2 h at an MOI of 1. RNA was isolated using the Innuprep RNA minikit 2.0 (Jena Analytik, Germany) with an additional DNAse digestion step (RNase-free DNase set; Qiagen, Germany). Quality and quantity of the total RNA samples were evaluated with the Tape Station 2200 (Agilent, USA) and the Nanodrop 1000 (Thermo Fisher Scientific, Germany), respectively. Stranded RNA libraries were then prepared from 1 µg total RNA using the TruSeq Stranded mRNA Prep Kit (Illumina, USA) following the manufacturer's protocol. Multiplexing of the samples was achieved using IDT–TruSeq RNA UD Indexes (Illumina, USA). The libraries were then loaded on a S1 Flowcell using the Xp Workflow and subjected to 100 cycles paired-end sequencing on the Illumina NovaSeq 6000 System.

Analysis of sequencing data. Our dataset is composed by 40 fastq files corresponding to reads one and two (paired-end sequencing) of the 20 samples of the project. Those 20 samples correspond to replicates one and two of the 10 different conditions. All these files can be found in the SRA repository (https://www.ncbi.nlm.nih.gov/sra/PRJNA681392). We used the galaxy-europe server (77) to map the fastq files and count the gene transcriptions; the following named functions are all included in the server and were used using the default parameters except where it is otherwise indicated. First, the quality of the fastq files was assessed using the function *FastQC* then the

adapter sequences were trimmed with the help of the function *Cutadapt* (78). This result was mapped to the human genome hg38 using the *RNA Star* (79) applied for pair-ended sequences, the "Length of the genomic sequence around annotated junctions" parameter was set to 50. From the RNA Star function, we obtained the bam files which were quality controlled and later used to look for gene counts with the *FeatureCount* function. We processed the reverse stranded bam files allowing for fragment counts but not multimapping. The minimum mapping quality per read was set to 10. Finally, we obtained the count files for each of the samples in the project.

DEG fold-change analysis. We analyzed the count files in R, using the *DESeq2* (80) and the *edgeR* (81) packages. The first step was to calculate the RPKM (Reads Per Kilobase Million) values for each gene, and discard those genes with an RPKM value lower than three. The remaining genes were processed to look for differentially expressed genes (DEG's). For this purpose, a *DESeq* object was created with the design formula *C. albicans* + antibody meaning that the antibody treatments were being analyzed while controlling for the *C. albicans* stimulus. Then, we created the results tables based on the contrasts of antibody-treatments vs ISO treatment, for each of the CEACAM antibodies, respectively.

PCA. The principal component analysis (PCA) was made directly with the function embedded in the *DESeq2* package, using the top 500 genes. The antibody treatment was marked as interest group.

Gene Ontology analysis. The Gene Ontology (GO) knowledgebase (geneontology.org) (82, 83) was used for analysis of gene lists derived from the analysis of RNA-sequencing data (DEGs, as described above) using the *Panther* tool (84). Analysis summary: Analysis Type: PANTHER Overrepresentation Test (Released 20200728), Annotation Version and Release Date: GO Ontology database DOI: 10.5281/zenodo.4081749 Released 2020-10-09, Analyzed List: upload_1 (Homo sapiens), Reference List: Homo sapiens (all genes in database), Test Type: Fisher's Exact Binomial, Correction: Calculate False Discovery Rate.

Heatmaps. The heatmap grouping was defined based on significantly enriched GO terms important for neutrophil functions from the GO analysis (see "Gene Ontology analysis" above). The heatmaps present the normalized count values of the mentioned genes averaged over two biological replicates. Normal distribution was assumed. The normalization was done using the *counts* function of the *DESeq2* package with the parameter normalization set to true. Furthermore, within each subpanel heatmap the values were scaled (to mean = 0 and standard deviation = 1) by row, in order to facilitate the comparison between conditions (however, these are no longer absolute values).

Subnetwork and Module analysis. The network of human protein-protein interactions has been established in the FungiWeb database (C.H. Luther, C.W. Remmele, T. Dandekar, T. Müller, and M. Dittrich, submitted for publication, http://fungiweb.bioapps.biozentrum.uni-wuerzburg.de) (85). This network contains protein-protein interactions, which have been collected and curated from experimental data sets from the International Molecular Exchange (IMEx) consortium (86) via PSICQUIC queries (87) and have been filtered and curated to focus on experimental interactions only. Furthermore, interactions have been scored analogously to the MINT-Database score (87), which reflects the quality and quantity of experimental information supporting each interaction. For integrated network analysis only high and highest quality interactions (score cutoff ≥ 0.75) have been used and a network comprising the largest connected component has been derived

with a total of 17.754 genes and 237.846 interactions. The integrated network analysis aims to identify the maximally responsive regions (modules) after stimulation within the large interactome network, according to the integrated gene expression profiles. Thus, for the network analysis, RNA-Seq data was first preprocessed by an in-house pipeline, and differential gene expression was analyzed using a generalized linear model as implemented in *DESeq2* (80), contrasting the different CEACAM-antibody treatments to the isotype antibody control. To obtain gene scores for the identification of responsive subnetworks a BUM (Beta Uniform Mixture) model has been fitted to the distribution of P-values using the routines in the *BioNet* package (88) choosing a stringent FDR (False Discovery Rate) threshold of 10^{-19} to focus only on the maximally responsive region. Based on the scored network optimally responsive modules have been identified using an exact approach, which, albeit computationally demanding, is capable (mathematically proven) to identify provably optimal modules (89). Visualization of the resulting subnetworks has been performed using *Cytoscape* (90). Enrichment analysis of the network modules has been performed with *g:Profiler* (91) against the background set of the genes in the interaction network, using default settings and focusing on KEGG (92) pathways only. The information for cell membrane and secreted localization were obtained from UniProt (93). All statistical analyses have been performed with the computational statistics framework *R* (version 3.6.3).

Systems biological modeling and network analysis. We created protein signaling networks for CC6 (Fig. 5) and CC1 (Fig. S1C). These networks combined the gene regulatory data from the RNA-sequencing analysis with data base knowledge of protein-protein interactions. First, the relevant genes were selected as those which reached an adjusted p-value lower than 0.05 and resulted in an expression of at least two-fold (red and blue nodes in Fig. 5 and Fig. S1C). In addition to these genes, we assembled a set of known interacting proteins of the CEACAM receptors (gray nodes in Fig. 5 and Fig. S1C). We calculated the edges between nodes from three different sources. The first source is the genie3 inference algorithm as presented in (94) and implemented in the *genie3* package in *R* (documentation at https://bioconductor.org/packages/release/bioc/html/GENIE3.html). This algorithm infers relations between nodes by creating a random forest classifier for each of the genes in the sample and the rest of the genes are used as variables. The algorithm then estimates the relevance of each gene for the classification of the target gene and based on this defines a weight that represent the plausibility of a connection between the two nodes. This value is not a statistical test and cannot be interpreted as such but it constitutes a ranking of the possible interactions between samples. For the CC6 network the threshold value was set to 0.45 and for CC1 the threshold value was set to 0.1. The interactions obtained by this method are marked in the network figures (Fig. 5 and Fig. S1C) as dashed lines. Also, we estimate the sign of the interactions (activating or inhibitory) by calculation a partial correlation between samples. This was done using the *pcor* function of the *ppcor* package in *R* (95). Because of the low sample number, the partial correlations do not reach statistical significance, for that reason we take a conservative approach and set as inhibitory interactions, only those that are lower than -0.3. The other two methods used are data base search based. We searched the string (96) and the biogrid (97) databases. The string database search was made directly on the string database website using the multiprotein search function. The results were pruned to show only experimental, databases or co-expression relations between nodes. We exported the results as a tab delimited table and use it as directed connections for our network.

Finally, we consulted the biogrid data base by downloading the *BIOGRID-ALL-4.2.191* interactions file and searching in *R* for the interactions that involved proteins or genes in our network. Interaction files are available from our website (https://www.biozentrum.uni-wuerzburg.de/bioinfo/computing/CEACAM/).

For the final assembly of the network, any duplicate interactions were removed. With the remaining interactions we assembled the networks using the *yEd* graphics program (freeware, https://www.yworks.com/products/yed). The gene ontology analysis of the DEG's within the network analysis was performed in *R* using the *TopGO* package (98). The annotation package *org.Hs.eg.db* from Bioconductor was used (99). The BP (Biological Process) ontology analysis was chosen. Two types of statistic measures were used for the enrichment analysis. Fischer's test, which is based on the gene count information, and a Kolmogorov-Smirnov-like test that relies on the gene scores, were made using the *classic* algorithm from the *TopGO* package. All the resulting *GO* terms and the respective test results for CC6 are provided in the Table S8. The results table is limited to the top 1000 results. The GO knowledgebase (geneontology.org) (39, 40) was used for analysis of those genes for which we had no expression data (extra nodes added for the network analysis, explained later). We used the Panther tool (41). Analysis summary: Analysis Type: PANTHER Overrepresentation Test (Released 20200728), Annotation Version and Release Date: GO Ontology database DOI: 10.5281/zenodo.4081749 Released 2020-10-09, Analyzed List: upload_1 (Homo sapiens), Reference List: Homo sapiens (all genes in database), Test Type: Fisher's Exact Binomial, Correction: Calculate False Discovery Rate.

Dynamical modeling of the involved response network considering CEACAM6, CEACAM3 and CEACAM1. We performed simulations of the networks in Fig. 5 using Jimena (100). Jimena is a software that enables the dynamical simulation of protein networks by modeling the Boolean state of nodes as a continuous hill function (100). This method is recognized to result in validated Boolean and semiquantitative models for systems biology in infections for transcriptome data (101-103). The nodes can have continuous activation values that range from zero to one. The sign of the connections remains as activating or inhibitory. For our simulations we created an extra node to stimulate the network and analyze its response to that stimulus. The extra node created is called PATHOGEN (for the pathogen *C. albicans*) and has an activating connection to each of the CEACAM nodes in the study (CEACAM1, CEACAM3 and CEACAM6). Also, to link the CEACAM receptors to the rest of the network we set interactions from the CEACAM1, CEACAM3 and CEACAM6 nodes to the most two differentially expressed genes in our RNA-seq analysis (*IL6* and *ACOD1*). For CEACAM3, only a connection to *IL6* was established since ACOD1 was not differentially expressed in that case.

Venn diagrams. Venn diagrams were calculated using the following online platform: http://bioinformatics.psb.ugent.be/webtools/Venn/. Lists of genes allocated to partitions of the respective diagrams were exported.

Data availability. Sequencing data are available under the following link: http://www.ncbi.nlm.nih.gov/bioproject/681392.

Statistics. Statistical analysis of all cell-based assays was performed using One-Way ANNOVA or Repeated Measures ANNOVA with Bonferroni post-test as indicated.

Funding. This work was supported by the German Research Foundation (Collaborative Research Center/Transregio 124 – FungiNet —Pathogenic fungi and their human host: Networks of Interaction, DFG project number 210879364, Projects B1, B2, and A5) to TD, MD, and HS, and ProChance 2018 – Programmlinie A1 (Förderkennzeichen 2.11.3-A1/218-01) to EK. The funders had no role in study design, data collection and interpretation, or the decision to submit the work for publication.

Acknowledgement. We thank Simone Tänzer, Moira Stark, Birgit Maranca-Hüwel, and Bärbel Gobs-Hevelke for their excellent technical support.

Figure Legends

Figure 1: Altered *C. albicans*-induced CXCL8 release by neutrophil treatment with anti-CEACAM6 antibody. Human neutrophils were left untreated or were incubated with 10 µg/ml mouse IgG1 isotype control antibody (clone MOPC-21), or monoclonal CEACAM-specific mouse monoclonal IgG1 antibodies for 45 min and were consecutively incubated with or without live *C. albicans* yeast cells (MOI 1) for 2 h. Antibody clones and their specific (cross-) reactivities for CEACAM1, CEACAM3 and CEACAM6 are indicated in (B) and (D). Cell culture supernatants were harvested and analyzed for CXCL8 concentrations in 2-7 independent experiments for the different treatment groups, represented by the single dots in the graphs. (A) CXCL8 release in untreated and isotype-treated neutrophils without and with *C. albicans* stimulation. (B) CXCL8 release in *C. albicans*-stimulated cells including all anti-CEACAM antibody treatments. (C) Samples pre-treated with isotype, B3-17 and 1H7-4B from (B) were plotted with linked samples from the same donor. Note the donor-independent relative increase of the CXCL8 response to *C. albicans* treatment after pre-stimulation with the CEACAM1- and the CEACAM6-monospecific antibody, respectively. (D) CXCL8 release after antibody treatments in absence of *C. albicans*. Statistical analyses were performed by One-Way ANOVA with Bonferroni post-test.

Figure 2: No alterations of *C. albicans* binding, ROS production and *C. albicans* killing by human neutrophils in response to anti-CEACAM antibodies. (A, B) Human neutrophils were stained for CD11b and left untreated or were incubated with 10 µg/ml isotype control antibody (clone MOPC-21), or monoclonal antibodies B3-17 (CC1), 308/3-3 (CC3), or 1H7-4B (CC6) for 45 min and were consecutively incubated with (A, B) or without (B) live, APC-labeled *C. albicans* yeast cells (MOI 1) for 20 min. Cells were then analyzed by flow cytometry for the percentage of *C. albicans*-bound neutrophils and the ROS production by DHR123. The graphs show the percentage of *C. albicans*-bound granulocytes (A), the logarithmized fluorescent signal of the DHR123 dye (B), and the respective means from two independent experiments. (C) 2×10^5 human neutrophils (2×10^6/ml) were left untreated or were incubated with 10 µg/ml isotype control antibody (clone MOPC-21), or monoclonal antibodies B3-17 (CC1), 308/3-3 (CC3), or 1H7-4B (CC6) for 45 min and were consecutively incubated with live *C. albicans* yeast cells (MOI 1) for 30 min. Viable *C. albicans* cells were quantified by XTT assay. The graph shows mean and SD

from three independent experiments (Statistics: Repeated Measures ANOVA; no significant differences).

Figure 3: Altered Ca-induced neutrophil transcriptional response by priming with anti-CEACAM antibodies. Human neutrophils were left untreated or were incubated with 10 µg/ml isotype control antibody (clone MOPC-21), or monoclonal antibodies B3-17 (CC1), 308/3-3 (CC3), or 1H7-4B (CC6) for 45 min and were consecutively incubated with or without live *C. albicans* yeast cells (MOI 1) for 2 h; mRNA was extracted and analyzed by sequencing. (A) PCA analysis of all antibody-treated samples in presence of *C. albicans* and IgG-treated control cells without *C. albicans* stimulation. Please refer to Figure S1A for a PCA including all samples. (B, C, D, E) Data presented in Figure 3A and Tables S1 and S3 were further analyzed for the CEACAM-specific responses by comparing shared differentially expressed genes (DEGs) from the different treatment groups. Only significantly regulated genes (adjusted p-value <0.05, fold-change at least ±2) were included. Note that for Venn diagrams, both, protein-coding and non-protein-coding genes were included. (B) Venn diagram of DEGs induced by anti-CEACAM antibody treatment and *C. albicans*-stimulation (IgG-treated neutrophils with *C. albicans* stimulation versus CC1-, CC3-, or CC6-treated neutrophils with *C. albicans* stimulation, respectively). Please refer to Table S3 for the DEGs within the partitions of the Venn diagram. (C) Venn diagram of DEGs regulated in a *C. albicans*-specific manner by CEACAM1 treatment alone (CC1) or in presence of *C. albicans* (CC1+Ca). Please refer to Table S4 for the classification of the DEGs into the partitions of the Venn diagram. (D) Venn diagram of DEGs regulated in a *C. albicans*-specific manner by CEACAM treatment alone (CC6) or in presence of *C. albicans* (CC6+Ca). Please refer to Table S5 for the classification of the DEGs into the partitions of the Venn diagram. (E) Venn diagram of differentially expressed genes (DEGs) induced by antibody stimulations alone (IgG-treated neutrophils versus CC1-, CC3-, or CC6-treated neutrophils, respectively). Please refer to Table S6 for the classification of the DEGs into the partitions of the Venn diagram.

Figure 4: CEACAM6-specific transcriptional responses of neutrophils in the presence of *C. albicans* and comparison to CEACAM1 and CEACAM3 antibody ligation experiments. Heat maps display DEGs after CEACAM6 (CC6) treatment in presence of *C. albicans* stimulation from major enriched GO categories (adjusted p-value < 0.05 and fold-change >±2; see also Table S1 for a complete list with fold-changes of all genes differentially expressed after CC6 treatment). The relative expression of each gene is shown for all treatment groups with *C. albicans* stimulation (untreated, UT; isotype control antibody-treated, IGG; B3-17-treated, CC1; 308/3-3-treated, CC3; 1H7-4B-treated, CC6). Each row was normalized (mean = 0) and scaled (standard deviation = 1); *also padj < 0.05 for CC1, ** also padj < 0.05 for CC3.

Figure 5. Integrated network analysis of CEACAM6-regulated genes in presence of *C. albicans*. Based on gene expression profile**s,** the optimally CEACAM6-responsive network module in presence of *C. albicans* has been identified. Subsequent KEGG enrichment analysis detected key signaling pathways of CEACAM6-antibody treated neutrophils stimulated with *C. albicans*, including apoptosis as well as NF-kappa-B and TLR signaling (pathway associated genes are highlighted and framed).

Figure 6: Cell function-centered network analysis of CEACAM6-regulated genes in presence of *C. albicans*. Signaling network assembled from the DEGs in CEACAM6-treated neutrophils in presence of *C. albicans* stimulation (blue and red nodes, Table S1) and known interactors of CEACAM family receptors (gray nodes). Interactions are inferred from the RNA-seq samples (dashed lines) or obtained from interaction databases (solid lines). Nodes belonging to significantly enriched GO terms important to neutrophil responses are clustered and framed.

Figure 7: Verification of the predicted altered apoptosis of human neutrophils after stimulation with *C. albicans* by CEACAM6 ligation. Human neutrophils were left untreated or were incubated with the following antibodies: isotype control (Iso), B3-17 (CC1), 308/3-3 (CC3) or 1H7-4B (CC6) for 45 min. Afterwards, cells were incubated with or without live *C. albicans* yeast cells (MOI 1) for 4 h (A, B, C) or for 24 h (D). Viability of human neutrophils after 4 h of *C. albicans*-stimulation was determined by Annexin V and propidium iodide staining with subsequent flow cytometric analysis. (A, C, D) graphs display the percentage of viable neutrophils (% of total neutrophils). (B) The graph displays the samples shown in (A) as percentage of viable neutrophils compared to untreated cells in each experiment (viable untreated cells = 100%) to highlight the donor-independent relative effect of CEACAM6 treatment on *C. albicans*-induced apoptosis. Statistical analysis was performed by Repeated Measures ANOVA and Bonferroni post-test.

Figure 8: *IL1B* transcription and IL-1β secretion *in vitro*. Human neutrophils were left untreated or were incubated with the following antibodies: isotype control (Iso), B3-17 (CC1), 308/3-3 (CC3) or 1H7-4B (CC6) for 45 min. Afterwards, cells were incubated with or without live *C. albicans* yeast cells (MOI 1) for 2 h (A) or 21 h (B, C). (A) mRNA was extracted after 2 h and analyzed by sequencing. Fold-changes of the *IL1B* gene expression compared to isotype treatment in absence or presence of *C. albicans* stimulation, respectively, are shown. Fold-changes with an adjusted p-value<0.05 are marked with an asterisk. (B, C) Supernatants were collected after 21 h and analyzed for IL-1β concentrations (sensitivity: 4 pg/ml). Statistical analysis was performed by Repeated Measures ANOVA and Bonferroni post-test; samples below the detection range were set to the detection limit for statistical analysis.

Figure 9: Predicted and experimentally measured IL-6 secretion in anti-CEACAM3-treated samples. (A) Sub-network of *IL1B* induction by IL6 signaling. The network shown is a subgraph from the network displayed in Figure 5. All paths between IL6 and *IL1B* up to 7 nodes long were extracted; dashed lines: inferred interactions from our network analysis, solid lines: interactions obtained from data bases. (B-D) Human neutrophils were left untreated or were incubated with the following antibodies: isotype control (Iso), B3-17 (CC1), 308/3-3 (CC3) or 1H7-4B (CC6) for 45 min. Afterwards, cells were incubated with or without live *C. albicans* yeast cells (MOI 1) for 2 h (B) or 21 h (C, D). (B) mRNA was extracted after 2 h and analyzed by sequencing. Fold-changes of the *IL6* gene expression compared to isotype treatment in absence or presence of *C. albicans* stimulation, respectively, are shown. Fold-changes with an adjusted p-value<0.05 are marked with an asterisk. (C, D) Supernatants were collected after 21 h and analyzed for IL-6 concentrations

(sensitivity: 2 pg/ml). Statistical analysis was performed by Repeated Measure ANOVA and Bonferroni post-test.

Supplemental Figure Legends

Figure S1: Additional analyses of transcriptomic data. (A) Principal component analysis (PCA) of all samples (untreated, UT; isotype control antibody-treated, Iso; B3-17-treated, CC1, 308/3-3-treated, CC3; 1H7-4B-treated, CC6) without (US) and with *C. albicans* stimulation (+Ca) presented in Figure 3. (B) Altered *C. albicans*-induced neutrophil transcriptional response after treatment with anti-CEACAM1 antibody. Heat maps display DEGs after CEACAM1 (CC1) treatment in presence of *C. albicans* from major enriched GO categories (adjusted p-value < 0.05 and fold-change >±2; see also Table S1 for a complete list with fold-changes of all DEGs). The relative expression of each gene is shown for all treatment groups with *C. albicans* stimulation (untreated, UT; isotype control antibody-treated, IGG; B3-17-treated, CC1; 308/3-3-treated, CC3; 1H7-4B-treated, CC6). Each row was normalized (mean = 0) and scaled (standard deviation = 1); *also padj < 0.05 for CC6, ** also padj < 0.05 for CC3. Note that "programmed cell death" and "secretion" were not among the enriched GO categories. (C) Signaling network assembled from the DEGs in CC1-treated neutrophils in presence of *C. albicans* stimulation (blue and red nodes, Table S1) and known interactors of CEACAM family receptors (gray nodes). Interactions are inferred from the RNA-seq samples (dashed lines) or obtained from interaction databases (solid lines). Nodes belonging to significantly enriched GO terms important to neutrophil responses are clustered and framed.

Figure S2. Result curves of the dynamical simulation of Figs. 5 and S1C. The whole networks around the CEACAM receptors and each protein activation pathway was modelled and considered in the dynamical simulation of the pathogen stimulation effects. For the simulations the extra node "PATHOGEN" (for pathogen *C. albicans*) was added to the network; this node is activating and linked to the CEACAM1 (A) and the CEACAM6 (B) node, respectively. The information flow was modeled using Hill functions. Selected trajectories are presented here.

Supplemental Tables

Table S1: Significantly differentially expressed genes in anti-CEACAM antibody treated neutrophils versus isotype-treated neutrophils in presence of *C. albicans* infection.
Differentially expressed genes (DEGs; fold-change >±2, adjusted p-value <0.05) from transcriptomic analysis shown in Fig. 3A are listed for the given comparisons. Empty cells signify that no significant differences for a fold-change of at least ±2-fold were found for the respective gene in the comparison. Numbers in brackets indicate the combined effect of C. albicans-induced changes (column 2) and their alteration by CEACAM1 or CEACAM6 antibody treatment (columns 3 and 5, respectively); synergistic positive co-regulation is indicated by blue numbers, negative co-regulation by red numbers and counter-regulation by gray numbers.

Table S2: Significantly differentially expressed genes with at least +/- 2-fold-change in CEACAM1-, CEACAM3-, and CEACAM6-treated neutrophils versus isotype-treated neutrophils without *C. albicans* stimulation.

Differentially expressed genes (DEGs; fold-change >±2, adjusted p-value <0.05) from transcriptomic analysis shown in Figs. 3E and S1A are listed for the given comparisons. Empty cells signify that no significant differences for a fold-change of at least ±2-fold were found for the respective gene in the comparison.

Table S3: Genes included in the partitions of the Venn diagram in Figure 2B.

Table S4: Genes includes in the partitions of the Venn diagram in Figure 2C.

Table S5: Genes includes in the partitions of the Venn diagram in Figure 2D.

Table S6: Genes includes in the partitions of the Venn diagram in Figure 2E

Table S7: Enriched pathways of the network analysis presented in Figure 5.

Table S8: Enriched cellular functions (Gene Ontology) of the network analysis presented in Figure 6.

References

1. Kullberg BJ, Arendrup MC. 2015. Invasive Candidiasis. N Engl J Med 373:1445-56.
2. Sonego F, Castanheira FV, Ferreira RG, Kanashiro A, Leite CA, Nascimento DC, Colon DF, Borges Vde F, Alves-Filho JC, Cunha FQ. 2016. Paradoxical Roles of the Neutrophil in Sepsis: Protective and Deleterious. Front Immunol 7:155.
3. Tamassia N, Bianchetto-Aguilera F, Arruda-Silva F, Gardiman E, Gasperini S, Calzetti F, Cassatella MA. 2018. Cytokine production by human neutrophils: Revisiting the "dark side of the moon". Eur J Clin Invest 48 Suppl 2:e12952.
4. Metzemaekers M, Gouwy M, Proost P. 2020. Neutrophil chemoattractant receptors in health and disease: double-edged swords. Cell Mol Immunol 17:433-450.
5. Schauer AE, Klassert TE, von Lachner C, Riebold D, Schneeweiss A, Stock M, Muller MM, Hammerschmidt S, Bufler P, Seifert U, Dietert K, Dinarello CA, Nold MF, Gruber AD, Nold-Petry CA, Slevogt H. 2017. IL-37 Causes Excessive Inflammation and Tissue Damage in Murine Pneumococcal Pneumonia. J Innate Immun 9:403-418.
6. Azcutia V, Parkos CA, Brazil JC. 2017. Role of negative regulation of immune signaling pathways in neutrophil function. J Leukoc Biol doi:10.1002/JLB.3MIR0917-374R.
7. Sadarangani M, Pollard AJ, Gray-Owen SD. 2011. Opa proteins and CEACAMs: pathways of immune engagement for pathogenic Neisseria. FEMS Microbiol Rev 35:498-514.
8. Singer BB, Opp L, Heinrich A, Schreiber F, Binding-Liermann R, Berrocal-Almanza LC, Heyl KA, Muller MM, Weimann A, Zweigner J, Slevogt H. 2014. Soluble CEACAM8 interacts with CEACAM1 inhibiting TLR2-triggered immune responses. PLoS One 9:e94106.
9. Slevogt H, Seybold J, Tiwari KN, Hocke AC, Jonatat C, Dietel S, Hippenstiel S, Singer BB, Bachmann S, Suttorp N, Opitz B. 2007. Moraxella catarrhalis is internalized in respiratory epithelial cells by a trigger-like mechanism and initiates a TLR2- and partly NOD1-dependent inflammatory immune response. Cell Microbiol 9:694-707.
10. Lu R, Pan H, Shively JE. 2012. CEACAM1 negatively regulates IL-1beta production in LPS activated neutrophils by recruiting SHP-1 to a SYK-TLR4-CEACAM1 complex. PLoS Pathog 8:e1002597.
11. Gray-Owen SD, Blumberg RS. 2006. CEACAM1: contact-dependent control of immunity. Nat Rev Immunol 6:433-46.
12. Klaile E, Muller MM, Schafer MR, Clauder AK, Feer S, Heyl KA, Stock M, Klassert TE, Zipfel PF, Singer BB, Slevogt H. 2017. Binding of Candida albicans to Human CEACAM1 and CEACAM6 Modulates the Inflammatory Response of Intestinal Epithelial Cells. mBio 8.
13. Singer BB, Scheffrahn I, Heymann R, Sigmundsson K, Kammerer R, Obrink B. 2002. Carcinoembryonic antigen-related cell adhesion molecule 1 expression and signaling in human, mouse, and rat leukocytes: evidence for replacement of the short cytoplasmic domain isoform by glycosylphosphatidylinositol-linked proteins in human leukocytes. J Immunol 168:5139-46.
14. Tchoupa AK, Schuhmacher T, Hauck CR. 2014. Signaling by epithelial members of the CEACAM family - mucosal docking sites for pathogenic bacteria. Cell Commun Signal 12:27.
15. Helfrich I, Singer BB. 2019. Size Matters: The Functional Role of the CEACAM1 Isoform Signature and Its Impact for NK Cell-Mediated Killing in Melanoma. Cancers (Basel) 11.
16. Muller MM, Singer BB, Klaile E, Obrink B, Lucka L. 2005. Transmembrane CEACAM1 affects integrin-dependent signaling and regulates extracellular matrix protein-specific morphology and migration of endothelial cells. Blood 105:3925-34.

17. Javaheri A, Kruse T, Moonens K, Mejias-Luque R, Debraekeleer A, Asche CI, Tegtmeyer N, Kalali B, Bach NC, Sieber SA, Hill DJ, Koniger V, Hauck CR, Moskalenko R, Haas R, Busch DH, Klaile E, Slevogt H, Schmidt A, Backert S, Remaut H, Singer BB, Gerhard M. 2016. Helicobacter pylori adhesin HopQ engages in a virulence-enhancing interaction with human CEACAMs. Nat Microbiol 2:16189.
18. Slevogt H, Zabel S, Opitz B, Hocke A, Eitel J, N'Guessan P D, Lucka L, Riesbeck K, Zimmermann W, Zweigner J, Temmesfeld-Wollbrueck B, Suttorp N, Singer BB. 2008. CEACAM1 inhibits Toll-like receptor 2-triggered antibacterial responses of human pulmonary epithelial cells. Nat Immunol 9:1270-8.
19. Kammerer R, Hahn S, Singer BB, Luo JS, von Kleist S. 1998. Biliary glycoprotein (CD66a), a cell adhesion molecule of the immunoglobulin superfamily, on human lymphocytes: structure, expression and involvement in T cell activation. Eur J Immunol 28:3664-74.
20. Singer BB, Klaile E, Scheffrahn I, Muller MM, Kammerer R, Reutter W, Obrink B, Lucka L. 2005. CEACAM1 (CD66a) mediates delay of spontaneous and Fas ligand-induced apoptosis in granulocytes. Eur J Immunol 35:1949-59.
21. Khairnar V, Duhan V, Maney SK, Honke N, Shaabani N, Pandyra AA, Seifert M, Pozdeev V, Xu HC, Sharma P, Baldin F, Marquardsen F, Merches K, Lang E, Kirschning C, Westendorf AM, Haussinger D, Lang F, Dittmer U, Kuppers R, Recher M, Hardt C, Scheffrahn I, Beauchemin N, Gothert JR, Singer BB, Lang PA, Lang KS. 2015. CEACAM1 induces B-cell survival and is essential for protective antiviral antibody production. Nat Commun 6:6217.
22. Khairnar V, Duhan V, Patil AM, Zhou F, Bhat H, Thoens C, Sharma P, Adomati T, Friendrich SK, Bezgovsek J, Dreesen JD, Wennemuth G, Westendorf AM, Zelinskyy G, Dittmer U, Hardt C, Timm J, Gothert JR, Lang PA, Singer BB, Lang KS. 2018. CEACAM1 promotes CD8(+) T cell responses and improves control of a chronic viral infection. Nat Commun 9:2561.
23. Bonsignore P, Kuiper JWP, Adrian J, Goob G, Hauck CR. 2019. CEACAM3-A Prim(at)e Invention for Opsonin-Independent Phagocytosis of Bacteria. Front Immunol 10:3160.
24. Sintsova A, Guo CX, Sarantis H, Mak TW, Glogauer M, Gray-Owen SD. 2018. Bcl10 synergistically links CEACAM3 and TLR-dependent inflammatory signalling. Cell Microbiol 20.
25. Heinrich A, Heyl KA, Klaile E, Muller MM, Klassert TE, Wiessner A, Fischer K, Schumann RR, Seifert U, Riesbeck K, Moter A, Singer BB, Bachmann S, Slevogt H. 2016. Moraxella catarrhalis induces CEACAM3-Syk-CARD9-dependent activation of human granulocytes. Cell Microbiol 18:1570-1582.
26. Gutbier B, Fischer K, Doehn JM, von Lachner C, Herr C, Klaile E, Frischmann U, Singer BB, Riesbeck K, Zimmermann W, Suttorp N, Bachmann S, Bals R, Witzenrath M, Slevogt H. 2015. Moraxella catarrhalis induces an immune response in the murine lung that is independent of human CEACAM5 expression and long-term smoke exposure. Am J Physiol Lung Cell Mol Physiol 309:L250-61.
27. Pils S, Kopp K, Peterson L, Delgado Tascon J, Nyffenegger-Jann NJ, Hauck CR. 2012. The adaptor molecule Nck localizes the WAVE complex to promote actin polymerization during CEACAM3-mediated phagocytosis of bacteria. PLoS One 7:e32808.
28. Sarantis H, Gray-Owen SD. 2012. Defining the roles of human carcinoembryonic antigen-related cellular adhesion molecules during neutrophil responses to Neisseria gonorrhoeae. Infect Immun 80:345-58.

29. Tegtmeyer N, Ghete TD, Schmitt V, Remmerbach T, Cortes MCC, Bondoc EM, Graf HL, Singer BB, Hirsch C, Backert S. 2020. Type IV secretion of Helicobacter pylori CagA into oral epithelial cells is prevented by the absence of CEACAM receptor expression. Gut Pathog 12:25.
30. Tegtmeyer N, Harrer A, Schmitt V, Singer BB, Backert S. 2019. Expression of CEACAM1 or CEACAM5 in AZ-521 cells restores the type IV secretion deficiency for translocation of CagA by Helicobacter pylori. Cell Microbiol 21:e12965.
31. Behrens IK, Busch B, Ishikawa-Ankerhold H, Palamides P, Shively JE, Stanners C, Chan C, Leung N, Gray-Owen S, Haas R. 2020. The HopQ-CEACAM Interaction Controls CagA Translocation, Phosphorylation, and Phagocytosis of Helicobacter pylori in Neutrophils. mBio 11.
32. Brewer ML, Dymock D, Brady RL, Singer BB, Virji M, Hill DJ. 2019. Fusobacterium spp. target human CEACAM1 via the trimeric autotransporter adhesin CbpF. J Oral Microbiol 11:1565043.
33. Pan H, Shively JE. 2010. Carcinoembryonic antigen-related cell adhesion molecule-1 regulates granulopoiesis by inhibition of granulocyte colony-stimulating factor receptor. Immunity 33:620-31.
34. Zhang Z, La Placa D, Nguyen T, Kujawski M, Le K, Li L, Shively JE. 2019. CEACAM1 regulates the IL-6 mediated fever response to LPS through the RP105 receptor in murine monocytes. BMC Immunol 20:7.
35. Xie Q, Brackenbury LS, Hill DJ, Williams NA, Qu X, Virji M. 2014. Moraxella catarrhalis adhesin UspA1-derived recombinant fragment rD-7 induces monocyte differentiation to CD14+CD206+ phenotype. PLoS One 9:e90999.
36. Skubitz KM, Campbell KD, Skubitz AP. 1996. CD66a, CD66b, CD66c, and CD66d each independently stimulate neutrophils. J Leukoc Biol 60:106-17.
37. Skubitz KM, Skubitz AP. 2008. Interdependency of CEACAM-1, -3, -6, and -8 induced human neutrophil adhesion to endothelial cells. J Transl Med 6:78.
38. Saalbach A, Arnhold J, Lessig J, Simon JC, Anderegg U. 2008. Human Thy-1 induces secretion of matrix metalloproteinase-9 and CXCL8 from human neutrophils. Eur J Immunol 38:1391-403.
39. Pellme S, Morgelin M, Tapper H, Mellqvist UH, Dahlgren C, Karlsson A. 2006. Localization of human neutrophil interleukin-8 (CXCL-8) to organelle(s) distinct from the classical granules and secretory vesicles. J Leukoc Biol 79:564-73.
40. Hatanaka E, Monteagudo PT, Marrocos MS, Campa A. 2006. Neutrophils and monocytes as potentially important sources of proinflammatory cytokines in diabetes. Clin Exp Immunol 146:443-7.
41. Hidalgo MA, Carretta MD, Teuber SE, Zarate C, Carcamo L, Concha, II, Burgos RA. 2015. fMLP-Induced IL-8 Release Is Dependent on NADPH Oxidase in Human Neutrophils. J Immunol Res 2015:120348.
42. Klaile E, Muller MM, Zubiria-Barrera C, Brehme S, Klassert TE, Stock M, Durotin A, Nguyen TD, Feer S, Singer BB, Zipfel PF, Rudolphi S, Jacobsen ID, Slevogt H. 2019. Unaltered Fungal Burden and Lethality in Human CEACAM1-Transgenic Mice During Candida albicans Dissemination and Systemic Infection. Front Microbiol 10:2703.
43. Schirbel A, Rebert N, Sadler T, West G, Rieder F, Wagener C, Horst A, Sturm A, de la Motte C, Fiocchi C. 2019. Mutual Regulation of TLR/NLR and CEACAM1 in the Intestinal Microvasculature: Implications for IBD Pathogenesis and Therapy. Inflamm Bowel Dis 25:294-305.
44. Bourgeois C, Kuchler K. 2012. Fungal pathogens-a sweet and sour treat for toll-like receptors. Front Cell Infect Microbiol 2:142.

45. Philip NH, Dillon CP, Snyder AG, Fitzgerald P, Wynosky-Dolfi MA, Zwack EE, Hu B, Fitzgerald L, Mauldin EA, Copenhaver AM, Shin S, Wei L, Parker M, Zhang J, Oberst A, Green DR, Brodsky IE. 2014. Caspase-8 mediates caspase-1 processing and innate immune defense in response to bacterial blockade of NF-kappaB and MAPK signaling. Proc Natl Acad Sci U S A 111:7385-90.
46. Fritsch M, Gunther SD, Schwarzer R, Albert MC, Schorn F, Werthenbach JP, Schiffmann LM, Stair N, Stocks H, Seeger JM, Lamkanfi M, Kronke M, Pasparakis M, Kashkar H. 2019. Caspase-8 is the molecular switch for apoptosis, necroptosis and pyroptosis. Nature 575:683-687.
47. Sarantis H, Gray-Owen SD. 2007. The specific innate immune receptor CEACAM3 triggers neutrophil bactericidal activities via a Syk kinase-dependent pathway. Cell Microbiol 9:2167-80.
48. Sintsova A, Sarantis H, Islam EA, Sun CX, Amin M, Chan CH, Stanners CP, Glogauer M, Gray-Owen SD. 2014. Global analysis of neutrophil responses to Neisseria gonorrhoeae reveals a self-propagating inflammatory program. PLoS Pathog 10:e1004341.
49. Schmitter T, Agerer F, Peterson L, Munzner P, Hauck CR. 2004. Granulocyte CEACAM3 is a phagocytic receptor of the innate immune system that mediates recognition and elimination of human-specific pathogens. J Exp Med 199:35-46.
50. Schmitter T, Pils S, Sakk V, Frank R, Fischer KD, Hauck CR. 2007. The granulocyte receptor carcinoembryonic antigen-related cell adhesion molecule 3 (CEACAM3) directly associates with Vav to promote phagocytosis of human pathogens. J Immunol 178:3797-805.
51. Schmitter T, Pils S, Weibel S, Agerer F, Peterson L, Buntru A, Kopp K, Hauck CR. 2007. Opa proteins of pathogenic neisseriae initiate Src kinase-dependent or lipid raft-mediated uptake via distinct human carcinoembryonic antigen-related cell adhesion molecule isoforms. Infect Immun 75:4116-26.
52. Hauck CR, Lorenzen D, Saas J, Meyer TF. 1997. An in vitro-differentiated human cell line as a model system to study the interaction of Neisseria gonorrhoeae with phagocytic cells. Infect Immun 65:1863-9.
53. Slaats J, Ten Oever J, van de Veerdonk FL, Netea MG. 2016. IL-1beta/IL-6/CRP and IL-18/ferritin: Distinct Inflammatory Programs in Infections. PLoS Pathog 12:e1005973.
54. Nijhuis J, Rensen SS, Slaats Y, van Dielen FM, Buurman WA, Greve JW. 2009. Neutrophil activation in morbid obesity, chronic activation of acute inflammation. Obesity (Silver Spring) 17:2014-8.
55. Muller MM, Klaile E, Vorontsova O, Singer BB, Obrink B. 2009. Homophilic adhesion and CEACAM1-S regulate dimerization of CEACAM1-L and recruitment of SHP-2 and c-Src. J Cell Biol 187:569-81.
56. Singer BB, Scheffrahn I, Obrink B. 2000. The tumor growth-inhibiting cell adhesion molecule CEACAM1 (C-CAM) is differently expressed in proliferating and quiescent epithelial cells and regulates cell proliferation. Cancer Res 60:1236-44.
57. Dittrich M, Mueller HM, Bauer H, Peirats-Llobet M, Rodriguez PL, Geilfus CM, Carpentier SC, Al Rasheid KAS, Kollist H, Merilo E, Herrmann J, Muller T, Ache P, Hetherington AM, Hedrich R. 2019. The role of Arabidopsis ABA receptors from the PYR/PYL/RCAR family in stomatal acclimation and closure signal integration. Nat Plants 5:1002-1011.
58. Han ZM, Huang HM, Sun YW. 2018. Effect of CEACAM-1 knockdown in human colorectal cancer cells. Oncol Lett 16:1622-1626.

59. N'Guessan PD, Vigelahn M, Bachmann S, Zabel S, Opitz B, Schmeck B, Hippenstiel S, Zweigner J, Riesbeck K, Singer BB, Suttorp N, Slevogt H. 2007. The UspA1 protein of Moraxella catarrhalis induces CEACAM-1-dependent apoptosis in alveolar epithelial cells. J Infect Dis 195:1651-60.
60. Cameron S, de Long LM, Hazar-Rethinam M, Topkas E, Endo-Munoz L, Cumming A, Gannon O, Guminski A, Saunders N. 2012. Focal overexpression of CEACAM6 contributes to enhanced tumourigenesis in head and neck cancer via suppression of apoptosis. Mol Cancer 11:74.
61. Chan CH, Camacho-Leal P, Stanners CP. 2007. Colorectal hyperplasia and dysplasia due to human carcinoembryonic antigen (CEA) family member expression in transgenic mice. PLoS One 2:e1353.
62. Duxbury MS, Matros E, Ito H, Zinner MJ, Ashley SW, Whang EE. 2004. Systemic siRNA-mediated gene silencing: a new approach to targeted therapy of cancer. Ann Surg 240:667-74; discussion 675-6.
63. Gaur P, Ranjan P, Sharma S, Patel JR, Bowzard JB, Rahman SK, Kumari R, Gangappa S, Katz JM, Cox NJ, Lal RB, Sambhara S, Lal SK. 2012. Influenza A virus neuraminidase protein enhances cell survival through interaction with carcinoembryonic antigen-related cell adhesion molecule 6 (CEACAM6) protein. J Biol Chem 287:15109-17.
64. Kolla V, Gonzales LW, Bailey NA, Wang P, Angampalli S, Godinez MH, Madesh M, Ballard PL. 2009. Carcinoembryonic cell adhesion molecule 6 in human lung: regulated expression of a multifunctional type II cell protein. Am J Physiol Lung Cell Mol Physiol 296:L1019-30.
65. Riley CJ, Engelhardt KP, Saldanha JW, Qi W, Cooke LS, Zhu Y, Narayan ST, Shakalya K, Croce KD, Georgiev IG, Nagle RB, Garewal H, Von Hoff DD, Mahadevan D. 2009. Design and activity of a murine and humanized anti-CEACAM6 single-chain variable fragment in the treatment of pancreatic cancer. Cancer Res 69:1933-40.
66. Tian C, Zhang B, Ge C. 2020. Effect of CEACAM6 silencing on the biological behavior of human gallbladder cancer cells. Oncol Lett 20:2677-2688.
67. Kanderova V, Hrusak O, Kalina T. 2010. Aberrantly expressed CEACAM6 is involved in the signaling leading to apoptosis of acute lymphoblastic leukemia cells. Exp Hematol 38:653-660 e1.
68. Aleandri M, Conte MP, Simonetti G, Panella S, Celestino I, Checconi P, Marazzato M, Longhi C, Goldoni P, Nicoletti M, Barnich N, Palamara AT, Schippa S, Nencioni L. 2015. Influenza A virus infection of intestinal epithelial cells enhances the adhesion ability of Crohn's disease associated Escherichia coli strains. PLoS One 10:e0117005.
69. Klaile E, Klassert TE, Scheffrahn I, Muller MM, Heinrich A, Heyl KA, Dienemann H, Grunewald C, Bals R, Singer BB, Slevogt H. 2013. Carcinoembryonic antigen (CEA)-related cell adhesion molecules are co-expressed in the human lung and their expression can be modulated in bronchial epithelial cells by non-typable Haemophilus influenzae, Moraxella catarrhalis, TLR3, and type I and II interferons. Respir Res 14:85.
70. Negroni A, Costanzo M, Vitali R, Superti F, Bertuccini L, Tinari A, Minelli F, Di Nardo G, Nuti F, Pierdomenico M, Cucchiara S, Stronati L. 2012. Characterization of adherent-invasive Escherichia coli isolated from pediatric patients with inflammatory bowel disease. Inflamm Bowel Dis 18:913-24.
71. Barnich N, Carvalho FA, Glasser AL, Darcha C, Jantscheff P, Allez M, Peeters H, Bommelaer G, Desreumaux P, Colombel JF, Darfeuille-Michaud A. 2007. CEACAM6 acts as a receptor for adherent-invasive E. coli, supporting ileal mucosa colonization in Crohn disease. J Clin Invest 117:1566-74.

72. Carvalho FA, Barnich N, Sivignon A, Darcha C, Chan CH, Stanners CP, Darfeuille-Michaud A. 2009. Crohn's disease adherent-invasive Escherichia coli colonize and induce strong gut inflammation in transgenic mice expressing human CEACAM. J Exp Med 206:2179-89.
73. Shikotra A, Choy DF, Siddiqui S, Arthur G, Nagarkar DR, Jia G, Wright AK, Ohri CM, Doran E, Butler CA, Hargadon B, Abbas AR, Jackman J, Wu LC, Heaney LG, Arron JR, Bradding P. 2017. A CEACAM6-High Airway Neutrophil Phenotype and CEACAM6-High Epithelial Cells Are Features of Severe Asthma. J Immunol 198:3307-3317.
74. Klaile E, Vorontsova O, Sigmundsson K, Muller MM, Singer BB, Ofverstedt LG, Svensson S, Skoglund U, Obrink B. 2009. The CEACAM1 N-terminal Ig domain mediates cis- and trans-binding and is essential for allosteric rearrangements of CEACAM1 microclusters. J Cell Biol 187:553-67.
75. Klassert TE, Brauer J, Holzer M, Stock M, Riege K, Zubiria-Barrera C, Muller MM, Rummler S, Skerka C, Marz M, Slevogt H. 2017. Differential Effects of Vitamins A and D on the Transcriptional Landscape of Human Monocytes during Infection. Sci Rep 7:40599.
76. Klassert TE, Hanisch A, Brauer J, Klaile E, Heyl KA, Mansour MK, Tam JM, Vyas JM, Slevogt H. 2014. Modulatory role of vitamin A on the Candida albicans-induced immune response in human monocytes. Med Microbiol Immunol 203:415-24.
77. Afgan E, Baker D, Batut B, van den Beek M, Bouvier D, Cech M, Chilton J, Clements D, Coraor N, Gruning BA, Guerler A, Hillman-Jackson J, Hiltemann S, Jalili V, Rasche H, Soranzo N, Goecks J, Taylor J, Nekrutenko A, Blankenberg D. 2018. The Galaxy platform for accessible, reproducible and collaborative biomedical analyses: 2018 update. Nucleic Acids Res 46:W537-W544.
78. Martin M. 2011. Cutadapt removes adapter sequences from high-throughput sequencing reads. 2011 17:3.
79. Dobin A, Davis CA, Schlesinger F, Drenkow J, Zaleski C, Jha S, Batut P, Chaisson M, Gingeras TR. 2013. STAR: ultrafast universal RNA-seq aligner. Bioinformatics 29:15-21.
80. Love MI, Huber W, Anders S. 2014. Moderated estimation of fold change and dispersion for RNA-seq data with DESeq2. Genome Biol 15:550.
81. Robinson MD, McCarthy DJ, Smyth GK. 2010. edgeR: a Bioconductor package for differential expression analysis of digital gene expression data. Bioinformatics 26:139-40.
82. Ashburner M, Ball CA, Blake JA, Botstein D, Butler H, Cherry JM, Davis AP, Dolinski K, Dwight SS, Eppig JT, Harris MA, Hill DP, Issel-Tarver L, Kasarskis A, Lewis S, Matese JC, Richardson JE, Ringwald M, Rubin GM, Sherlock G. 2000. Gene ontology: tool for the unification of biology. The Gene Ontology Consortium. Nat Genet 25:25-9.
83. The Gene Ontology C. 2019. The Gene Ontology Resource: 20 years and still GOing strong. Nucleic Acids Res 47:D330-D338.
84. Mi H, Muruganujan A, Ebert D, Huang X, Thomas PD. 2019. PANTHER version 14: more genomes, a new PANTHER GO-slim and improvements in enrichment analysis tools. Nucleic Acids Res 47:D419-D426.
85. Remmele CW, Luther CH, Balkenhol J, Dandekar T, Muller T, Dittrich MT. 2015. Integrated inference and evaluation of host-fungi interaction networks. Front Microbiol 6:764.
86. Orchard S, Kerrien S, Abbani S, Aranda B, Bhate J, Bidwell S, Bridge A, Briganti L, Brinkman FS, Cesareni G, Chatr-aryamontri A, Chautard E, Chen C, Dumousseau M, Goll J, Hancock RE, Hannick LI, Jurisica I, Khadake J, Lynn DJ, Mahadevan U, Perfetto L, Raghunath A, Ricard-Blum S, Roechert B, Salwinski L, Stumpflen V, Tyers M, Uetz P, Xenarios I, Hermjakob H. 2012. Protein interaction data curation: the International Molecular Exchange (IMEx) consortium. Nat Methods 9:345-50.

87. Aranda B, Blankenburg H, Kerrien S, Brinkman FS, Ceol A, Chautard E, Dana JM, De Las Rivas J, Dumousseau M, Galeota E, Gaulton A, Goll J, Hancock RE, Isserlin R, Jimenez RC, Kerssemakers J, Khadake J, Lynn DJ, Michaut M, O'Kelly G, Ono K, Orchard S, Prieto C, Razick S, Rigina O, Salwinski L, Simonovic M, Velankar S, Winter A, Wu G, Bader GD, Cesareni G, Donaldson IM, Eisenberg D, Kleywegt GJ, Overington J, Ricard-Blum S, Tyers M, Albrecht M, Hermjakob H. 2011. PSICQUIC and PSISCORE: accessing and scoring molecular interactions. Nat Methods 8:528-9.

88. Beisser D, Klau GW, Dandekar T, Muller T, Dittrich MT. 2010. BioNet: an R-Package for the functional analysis of biological networks. Bioinformatics 26:1129-30.

89. Dittrich MT, Klau GW, Rosenwald A, Dandekar T, Muller T. 2008. Identifying functional modules in protein-protein interaction networks: an integrated exact approach. Bioinformatics 24:i223-31.

90. Shannon P, Markiel A, Ozier O, Baliga NS, Wang JT, Ramage D, Amin N, Schwikowski B, Ideker T. 2003. Cytoscape: a software environment for integrated models of biomolecular interaction networks. Genome Res 13:2498-504.

91. Raudvere U, Kolberg L, Kuzmin I, Arak T, Adler P, Peterson H, Vilo J. 2019. g:Profiler: a web server for functional enrichment analysis and conversions of gene lists (2019 update). Nucleic Acids Res 47:W191-W198.

92. Kanehisa M, Furumichi M, Tanabe M, Sato Y, Morishima K. 2017. KEGG: new perspectives on genomes, pathways, diseases and drugs. Nucleic Acids Res 45:D353-D361.

93. UniProt C. 2019. UniProt: a worldwide hub of protein knowledge. Nucleic Acids Res 47:D506-D515.

94. Huynh-Thu VA, Irrthum A, Wehenkel L, Geurts P. 2010. Inferring regulatory networks from expression data using tree-based methods. PLoS One 5.

95. Kim S. 2015. ppcor: An R Package for a Fast Calculation to Semi-partial Correlation Coefficients. Commun Stat Appl Methods 22:665-674.

96. Szklarczyk D, Gable AL, Lyon D, Junge A, Wyder S, Huerta-Cepas J, Simonovic M, Doncheva NT, Morris JH, Bork P, Jensen LJ, Mering CV. 2019. STRING v11: protein-protein association networks with increased coverage, supporting functional discovery in genome-wide experimental datasets. Nucleic Acids Res 47:D607-D613.

97. Stark C, Breitkreutz BJ, Reguly T, Boucher L, Breitkreutz A, Tyers M. 2006. BioGRID: a general repository for interaction datasets. Nucleic Acids Res 34:D535-9.

98. Alexa A, Rahnenfuhrer J. 2020. Enrichment Analysis for Gene Ontology. R package version 2.42.0., https://bioconductor.org/packages/release/bioc/html/topGO.html.

99. Carlson M. 2019. org.Hs.eg.db: Genome wide annotation for Human. R package version 3.8.2., https://bioconductor.org/packages/release/data/annotation/html/org.Hs.eg.db.html.

100. Karl S, Dandekar T. 2013. Jimena: efficient computing and system state identification for genetic regulatory networks. BMC Bioinformatics 14:306.

101. Yang M, Rajeeve K, Rudel T, Dandekar T. 2019. Comprehensive Flux Modeling of Chlamydia trachomatis Proteome and qRT-PCR Data Indicate Biphasic Metabolic Differences Between Elementary Bodies and Reticulate Bodies During Infection. Front Microbiol 10:2350.

102. Srivastava M, Bencurova E, Gupta SK, Weiss E, Loffler J, Dandekar T. 2019. Aspergillus fumigatus Challenged by Human Dendritic Cells: Metabolic and Regulatory Pathway Responses Testify a Tight Battle. Front Cell Infect Microbiol 9:168.

103. Cecil A, Gentschev I, Adelfinger M, Dandekar T, Szalay AA. 2019. Vaccinia virus injected human tumors: oncolytic virus efficiency predicted by antigen profiling analysis fitted boolean models. Bioengineered 10:190-196.

Figure 1

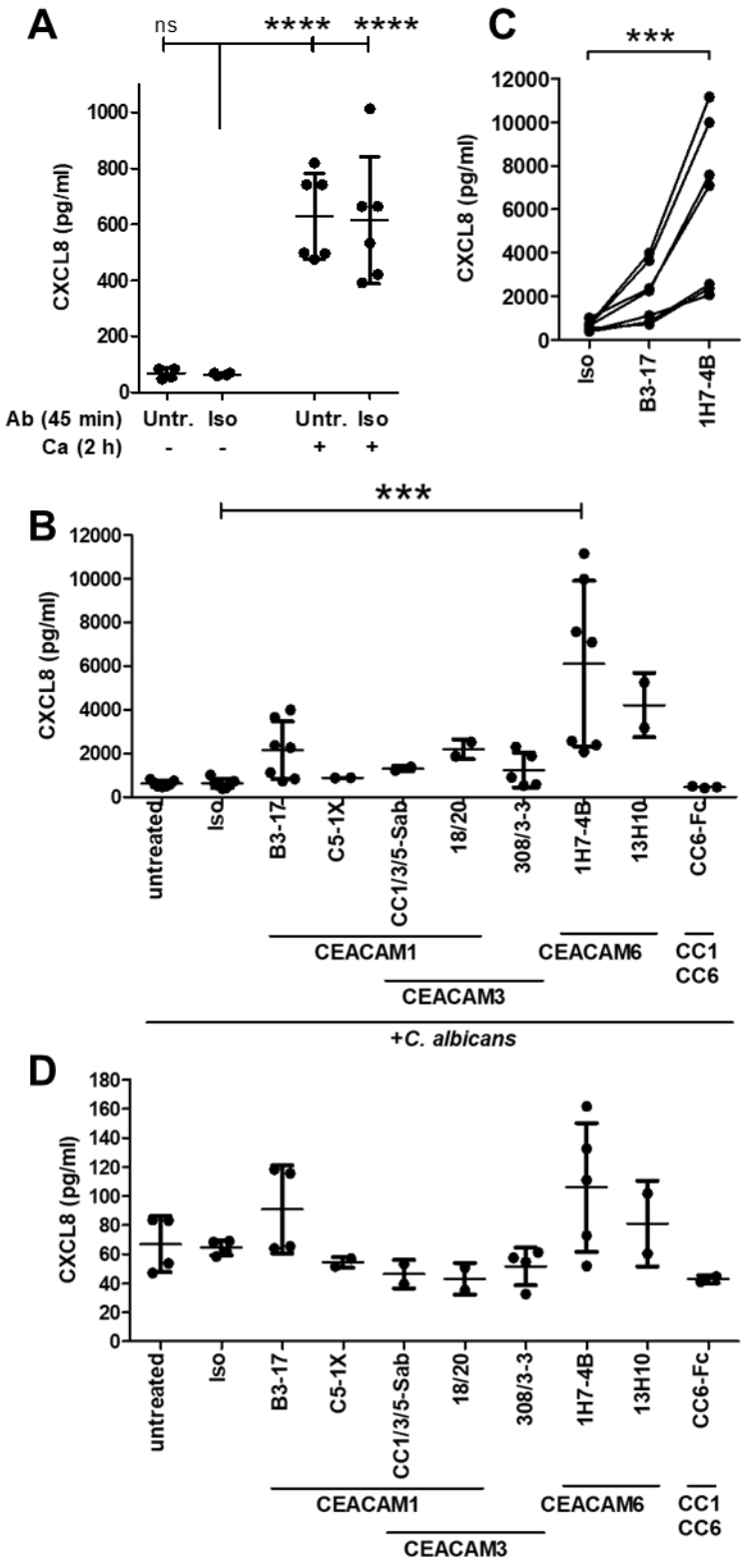

Figure 1: Altered *C. albicans*-induced CXCL8 release by neutrophil treatment with anti-CEACAM6 antibody. Human neutrophils were left untreated or were incubated with 10 µg/ml mouse IgG1 isotype control antibody (clone MOPC-21), or monoclonal CEACAM-specific mouse

monoclonal IgG1 antibodies for 45 min and were consecutively incubated with or without live *C. albicans* yeast cells (MOI 1) for 2 h. Antibody clones and their specific (cross-) reactivities for CEACAM1, CEACAM3 and CEACAM6 are indicated in (B) and (D). Cell culture supernatants were harvested and analyzed for CXCL8 concentrations in 2-7 independent experiments for the different treatment groups, represented by the single dots in the graphs. (A) CXCL8 release in untreated and isotype-treated neutrophils without and with *C. albicans* stimulation. (B) CXCL8 release in *C. albicans*-stimulated cells including all anti-CEACAM antibody treatments. (C) Samples pre-treated with isotype, B3-17 and 1H7-4B from (B) were plotted with linked samples from the same donor. Note the donor-independent relative increase of the CXCL8 response to *C. albicans* treatment after pre-stimulation with the CEACAM1- and the CEACAM6-monospecific antibody, respectively. (D) CXCL8 release after antibody treatments in absence of *C. albicans*. Statistical analyses were performed by One-Way ANOVA with Bonferroni post-test.

Figure 2

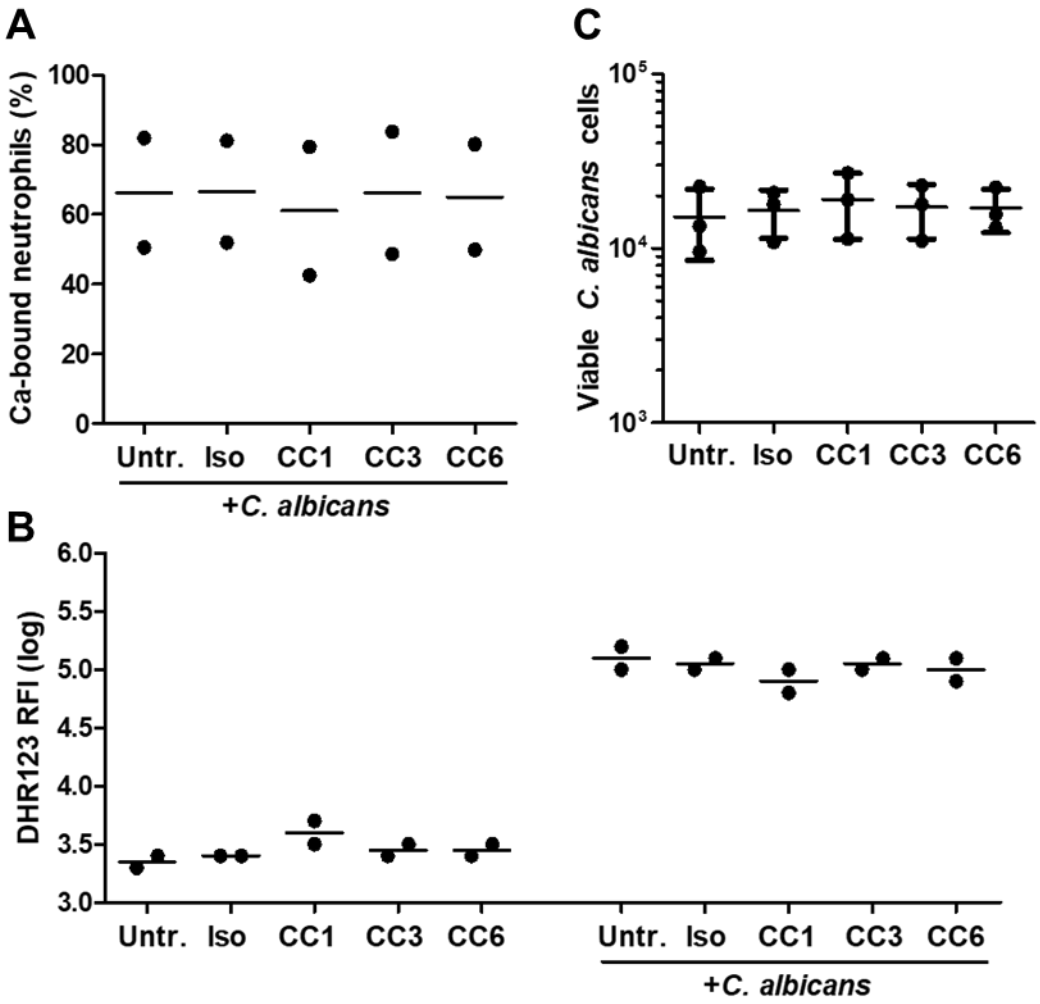

Figure 2: No alterations of *C. albicans* binding, ROS production and *C. albicans* killing by human neutrophils in response to anti-CEACAM antibodies. (A, B) Human neutrophils were stained for CD11b and left untreated or were incubated with 10 µg/ml isotype control antibody (clone MOPC-21), or monoclonal antibodies B3-17 (CC1), 308/3-3 (CC3), or 1H7-4B (CC6) for 45 min and were consecutively incubated with (A, B) or without (B) live, APC-labeled *C. albicans* yeast cells (MOI 1) for 20 min. Cells were then analyzed by flow cytometry for the percentage of *C. albicans*-bound neutrophils and the ROS production by DHR123. The graphs show the percentage of *C. albicans*-bound granulocytes (A), the logarithmized fluorescent signal of the DHR123 dye (B), and the respective means from two independent experiments. (C) 2×10^5 human neutrophils (2×10^6/ml) were left untreated or were incubated with 10 µg/ml isotype control antibody (clone MOPC-21), or monoclonal antibodies B3-17 (CC1), 308/3-3 (CC3), or 1H7-4B (CC6) for 45 min and were consecutively incubated with live *C. albicans* yeast cells (MOI 1) for 30 min. Viable *C. albicans* cells were quantified by XTT assay. The graph shows mean and SD from three independent experiments (Statistics: Repeated Measures ANOVA; no significant differences).

Figure 3

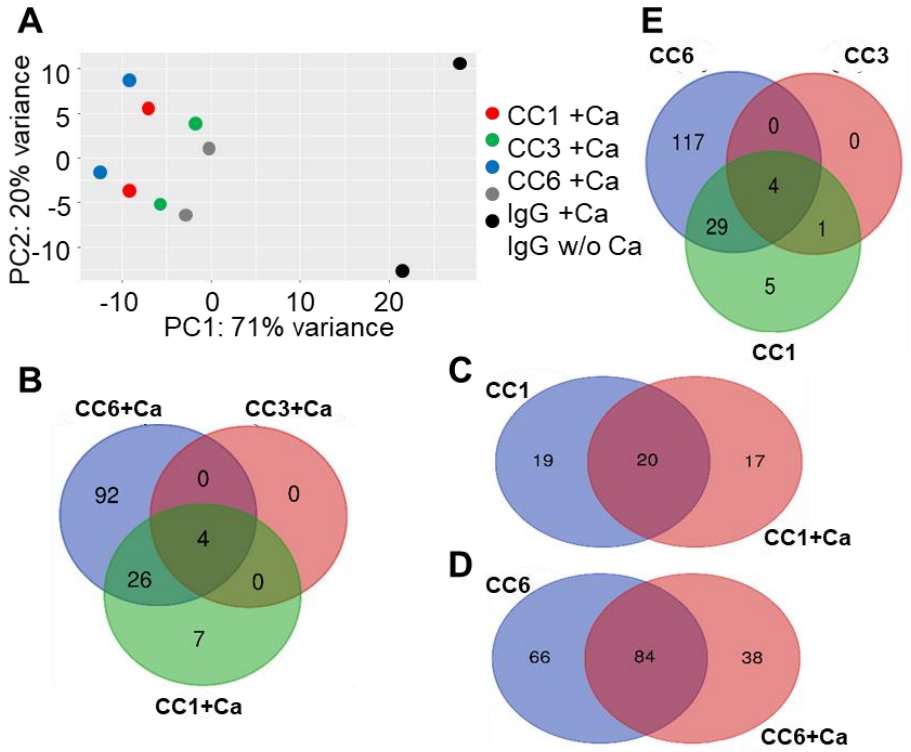

Figure 3: Altered Ca-induced neutrophil transcriptional response by priming with anti-CEACAM antibodies. Human neutrophils were left untreated or were incubated with 10 µg/ml isotype control antibody (clone MOPC-21), or monoclonal antibodies B3-17 (CC1), 308/3-3 (CC3), or 1H7-4B (CC6) for 45 min and were consecutively incubated with or without live *C. albicans* yeast cells (MOI 1) for 2 h; mRNA was extracted and analyzed by sequencing. (A) PCA analysis of all antibody-treated samples in presence of *C. albicans* and IgG-treated control cells without *C. albicans* stimulation. Please refer to Figure S1A for a PCA including all samples. (B, C, D, E) Data presented in Figure 3A and Tables S1 and S3 were further analyzed for the CEACAM-specific responses by comparing shared differentially expressed genes (DEGs) from the different treatment groups. Only significantly regulated genes (adjusted p-value <0.05, fold-change at least ±2) were included. Note that for Venn diagrams, both, protein-coding and non-protein-coding genes were included. (B) Venn diagram of DEGs induced by anti-CEACAM antibody treatment and *C. albicans*-stimulation (IgG-treated neutrophils with *C. albicans* stimulation versus CC1-, CC3-, or CC6-treated neutrophils with *C. albicans* stimulation, respectively). Please refer to Table S3 for the DEGs within the partitions of the Venn diagram. (C) Venn diagram of DEGs regulated in a *C. albicans*-specific manner by CEACAM1 treatment alone (CC1) or in presence of *C. albicans* (CC1+Ca). Please refer to Table S4 for the classification of the DEGs into the partitions of the Venn diagram. (D) Venn diagram of DEGs regulated in a *C. albicans*-specific manner by CEACAM treatment alone (CC6) or in presence of *C. albicans* (CC6+Ca). Please refer to Table S5 for the classification of the DEGs into the partitions of the Venn diagram. (E) Venn diagram of differentially expressed genes (DEGs) induced by antibody stimulations alone (IgG-treated neutrophils versus CC1-, CC3-, or CC6-treated neutrophils, respectively). Please refer to Table S6 for the classification of the DEGs into the partitions of the Venn diagram.

Figure 4

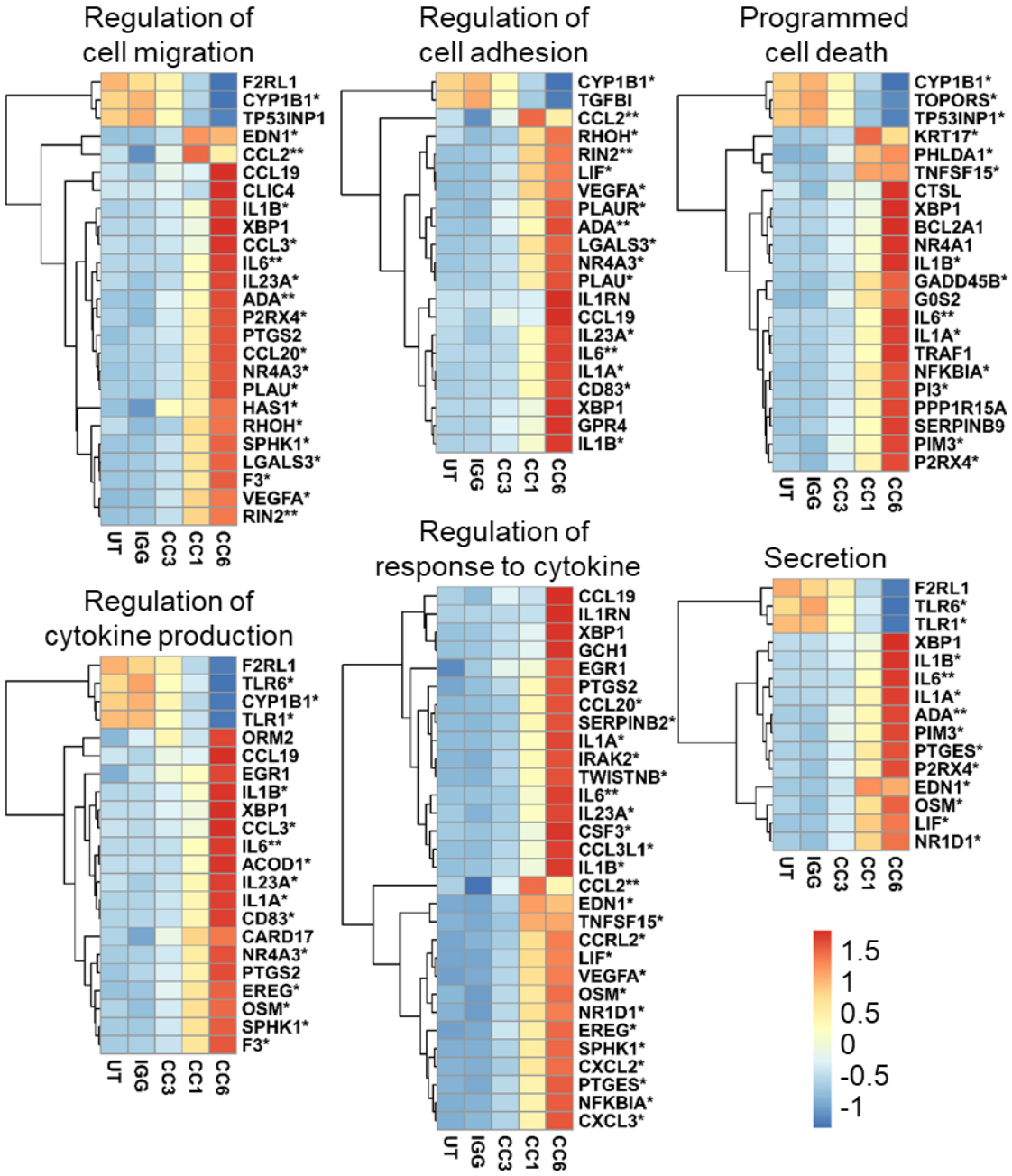

Figure 4: CEACAM6-specific transcriptional responses of neutrophils in the presence of *C. albicans* and comparison to CEACAM1 and CEACAM3 antibody ligation experiments. Heat maps display DEGs after CEACAM6 (CC6) treatment in presence of *C. albicans* stimulation from major enriched GO categories (adjusted p-value < 0.05 and fold-change >±2; see also Table S1 for a complete list with fold-changes of all genes differentially expressed after CC6 treatment). The relative expression of each gene is shown for all treatment groups with *C. albicans* stimulation (untreated, UT; isotype control antibody-treated, IGG; B3-17-treated, CC1; 308/3-3-treated, CC3; 1H7-4B-treated, CC6). Each row was normalized (mean = 0) and scaled (standard deviation = 1); *also padj < 0.05 for CC1, ** also padj < 0.05 for CC3.

Figure 5

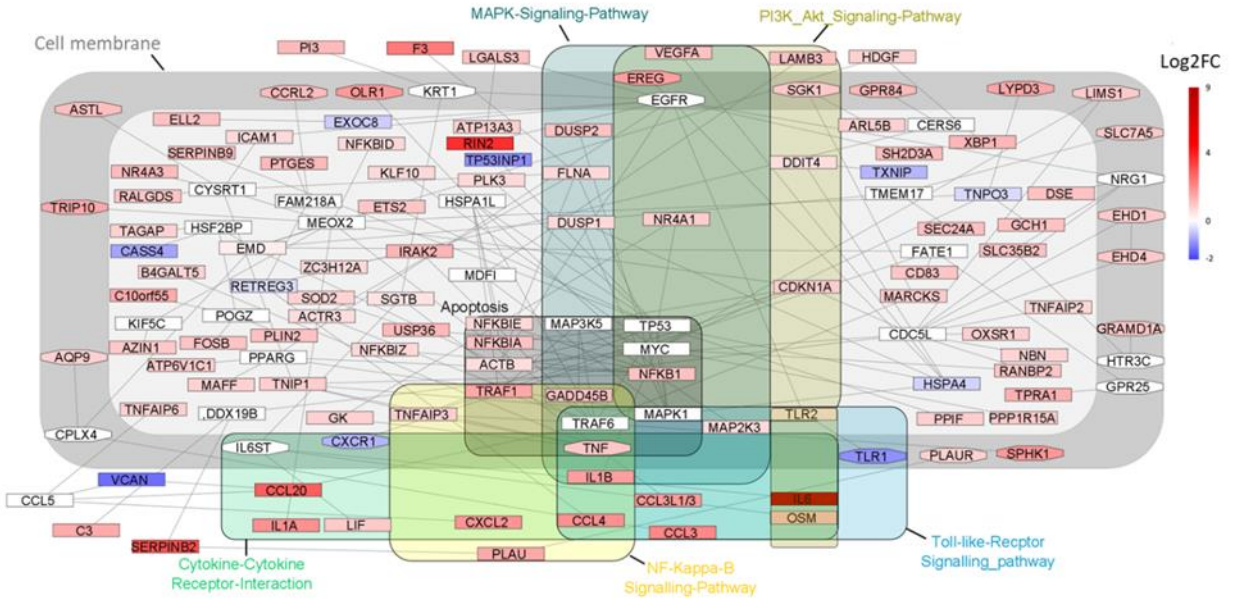

Figure 5. Integrated network analysis of CEACAM6-regulated genes in presence of *C. albicans*. Based on gene expression profile**s,** the optimally CEACAM6-responsive network module in presence of *C. albicans* has been identified. Subsequent KEGG enrichment analysis detected key signaling pathways of CEACAM6-antibody treated neutrophils stimulated with *C. albicans*, including apoptosis as well as NF-kappa-B and TLR signaling (pathway associated genes are highlighted and framed).

Figure 6

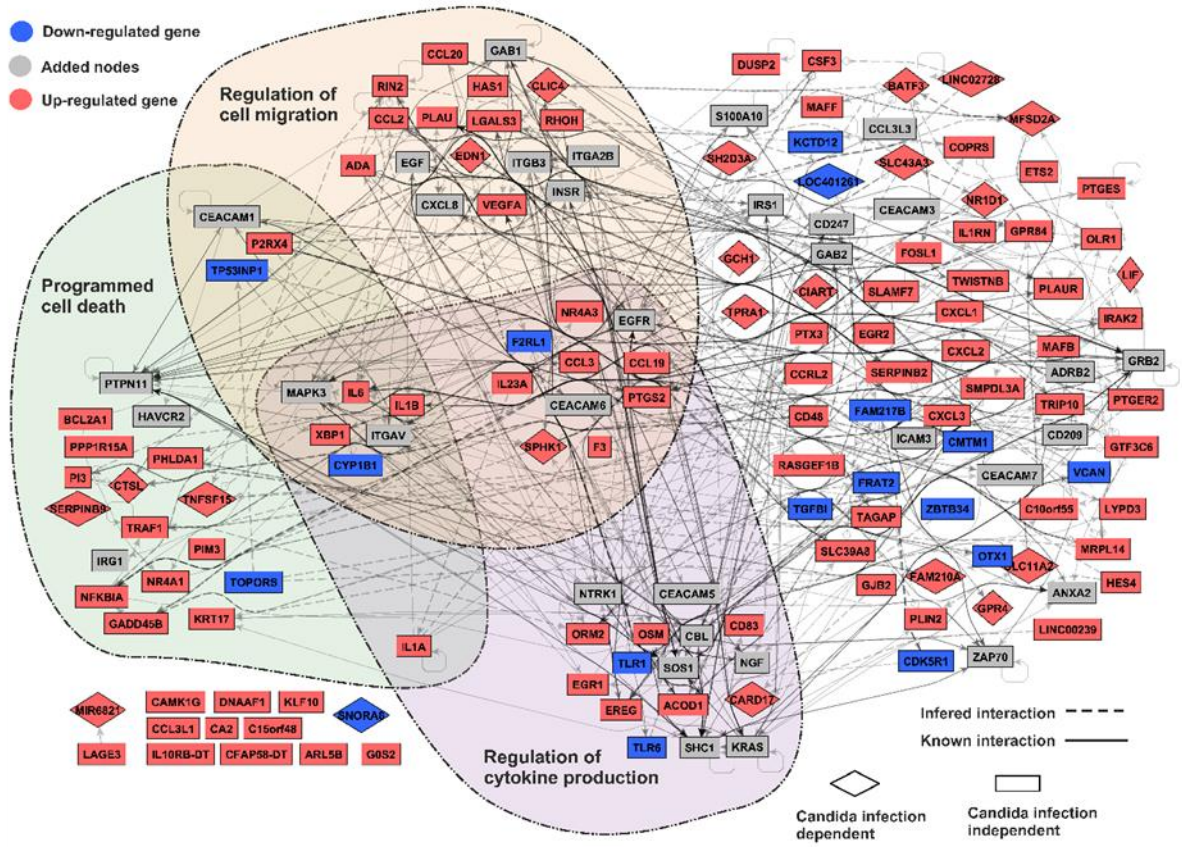

Figure 6: Cell function-centered network analysis of CEACAM6-regulated genes in presence of *C. albicans*. Signaling network assembled from the DEGs in CEACAM6-treated neutrophils in presence of *C. albicans* stimulation (blue and red nodes, Table S1) and known interactors of CEACAM family receptors (gray nodes). Interactions are inferred from the RNA-seq samples (dashed lines) or obtained from interaction databases (solid lines). Nodes belonging to significantly enriched GO terms important to neutrophil responses are clustered and framed.

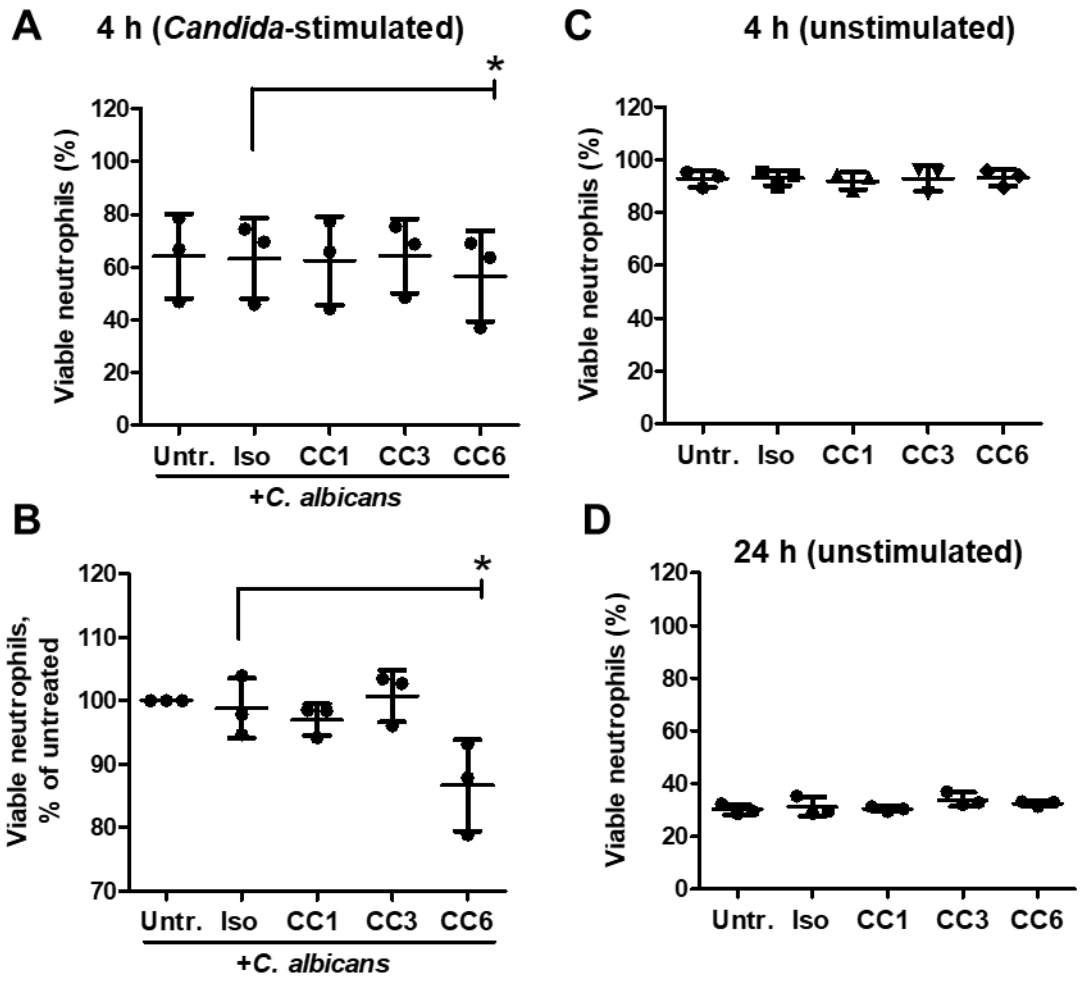

Figure 7: Verification of the predicted altered apoptosis of human neutrophils after stimulation with *C. albicans* by CEACAM6 ligation. Human neutrophils were left untreated or were incubated with the following antibodies: isotype control (Iso), B3-17 (CC1), 308/3-3 (CC3) or 1H7-4B (CC6) for 45 min. Afterwards, cells were incubated with or without live *C. albicans* yeast cells (MOI 1) for 4 h (A, B, C) or for 24 h (D). Viability of human neutrophils after 4 h of *C. albicans*-stimulation was determined by Annexin V and propidium iodide staining with subsequent flow cytometric analysis. (A, C, D) graphs display the percentage of viable neutrophils (% of total neutrophils). (B) The graph displays the samples shown in (A) as percentage of viable neutrophils compared to untreated cells in each experiment (viable untreated cells = 100%) to highlight the donor-independent relative effect of CEACAM6 treatment on *C. albicans*-induced apoptosis. Statistical analysis was performed by Repeated Measures ANOVA and Bonferroni post-test.

Figure 8

A

	Treatment		
	CC1	CC3	CC6
Fold-change IL1B without Candida stimulation	2.42*	1.62	6.49*
Fold-change IL1B with Candida stimulation (2.25* fold-change by candida alone)	1.99*	1.38	4.64*

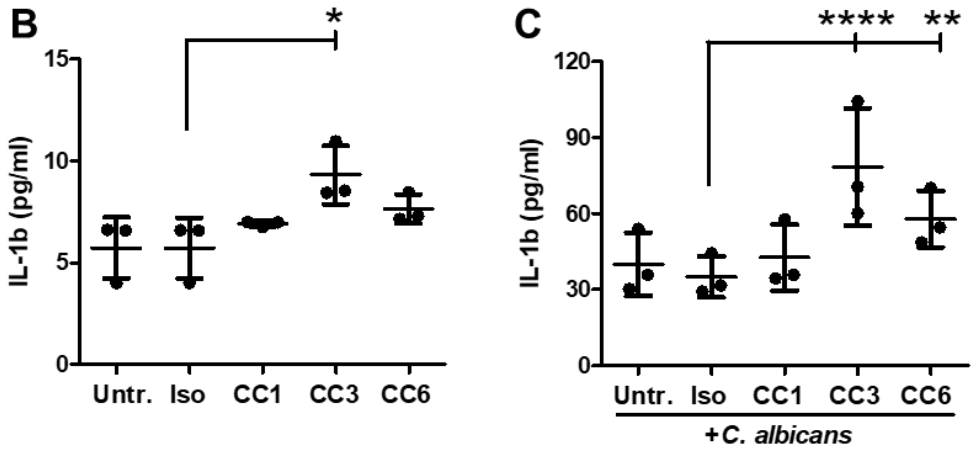

Figure 8: *IL1B* transcription and IL-1β secretion *in vitro*. Human neutrophils were left untreated or were incubated with the following antibodies: isotype control (Iso), B3-17 (CC1), 308/3-3 (CC3) or 1H7-4B (CC6) for 45 min. Afterwards, cells were incubated with or without live *C. albicans* yeast cells (MOI 1) for 2 h (A) or 21 h (B, C). (A) mRNA was extracted after 2 h and analyzed by sequencing. Fold-changes of the *IL1B* gene expression compared to isotype treatment in absence or presence of *C. albicans* stimulation, respectively, are shown. Fold-changes with an adjusted p-value<0.05 are marked with an asterisk. (B, C) Supernatants were collected after 21 h and analyzed for IL-1β concentrations (sensitivity: 4 pg/ml). Statistical analysis was performed by Repeated Measures ANOVA and Bonferroni post-test; samples below the detection range were set to the detection limit for statistical analysis.

Figure 9

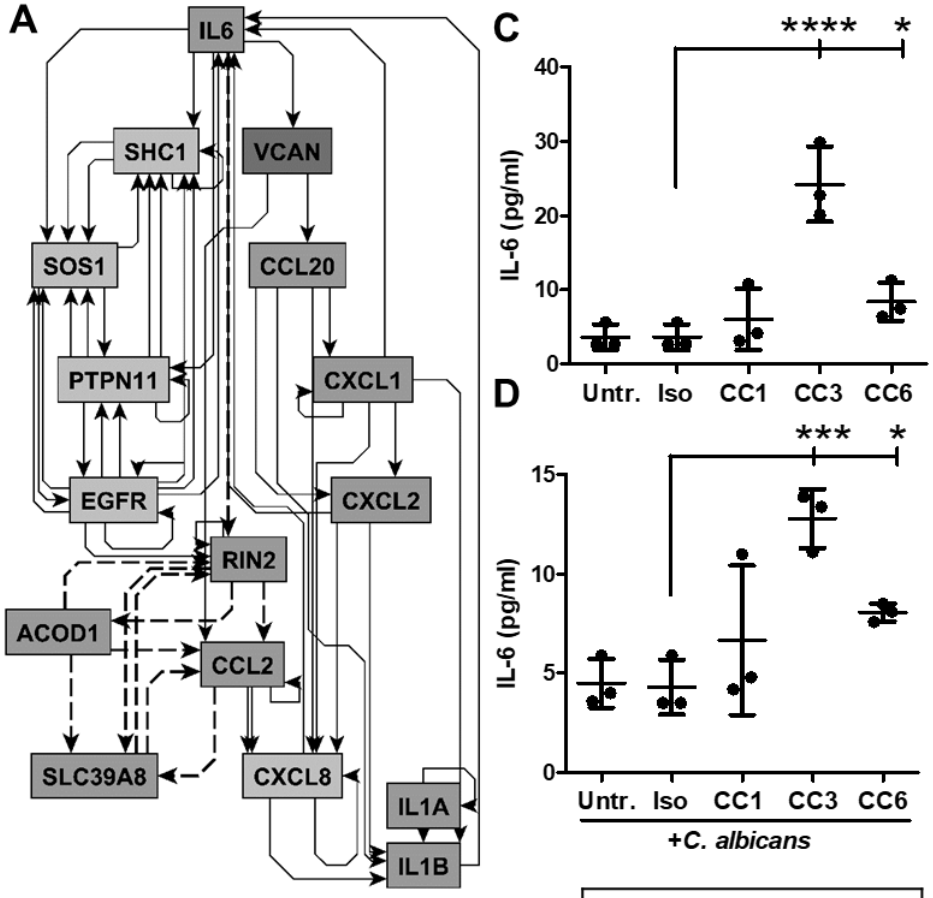

B

	Treatment		
	CC1	CC3	CC6
Fold-change IL6 without Candida stimulation	1973*	318*	3088*
Fold-change IL6 with Candida stimulation (1.15-fold-change by candida alone)	397*	48*	849*

Figure 9: Predicted and experimentally measured IL-6 secretion in anti-CEACAM3-treated samples. (A) Sub-network of *IL1B* induction by IL6 signaling. The network shown is a subgraph from the network displayed in Figure 5. All paths between IL6 and *IL1B* up to 7 nodes long were extracted; dashed lines: inferred interactions from our network analysis, solid lines: interactions obtained from data bases. (B-D) Human neutrophils were left untreated or were incubated with the following antibodies: isotype control (Iso), B3-17 (CC1), 308/3-3 (CC3) or 1H7-4B (CC6) for 45 min. Afterwards, cells were incubated with or without live *C. albicans* yeast cells (MOI 1) for 2 h (B) or 21 h (C, D). (B) mRNA was extracted after 2 h and analyzed by sequencing. Fold-changes of the *IL6* gene expression compared to isotype treatment in absence or presence of *C. albicans* stimulation, respectively, are shown. Fold-changes with an adjusted p-value<0.05 are marked with an asterisk. (C, D) Supernatants were collected after 21 h and analyzed for IL-6 concentrations (sensitivity: 2 pg/ml). Statistical analysis was performed by Repeated Measure ANOVA and Bonferroni post-test.

Supplemental Figure 1

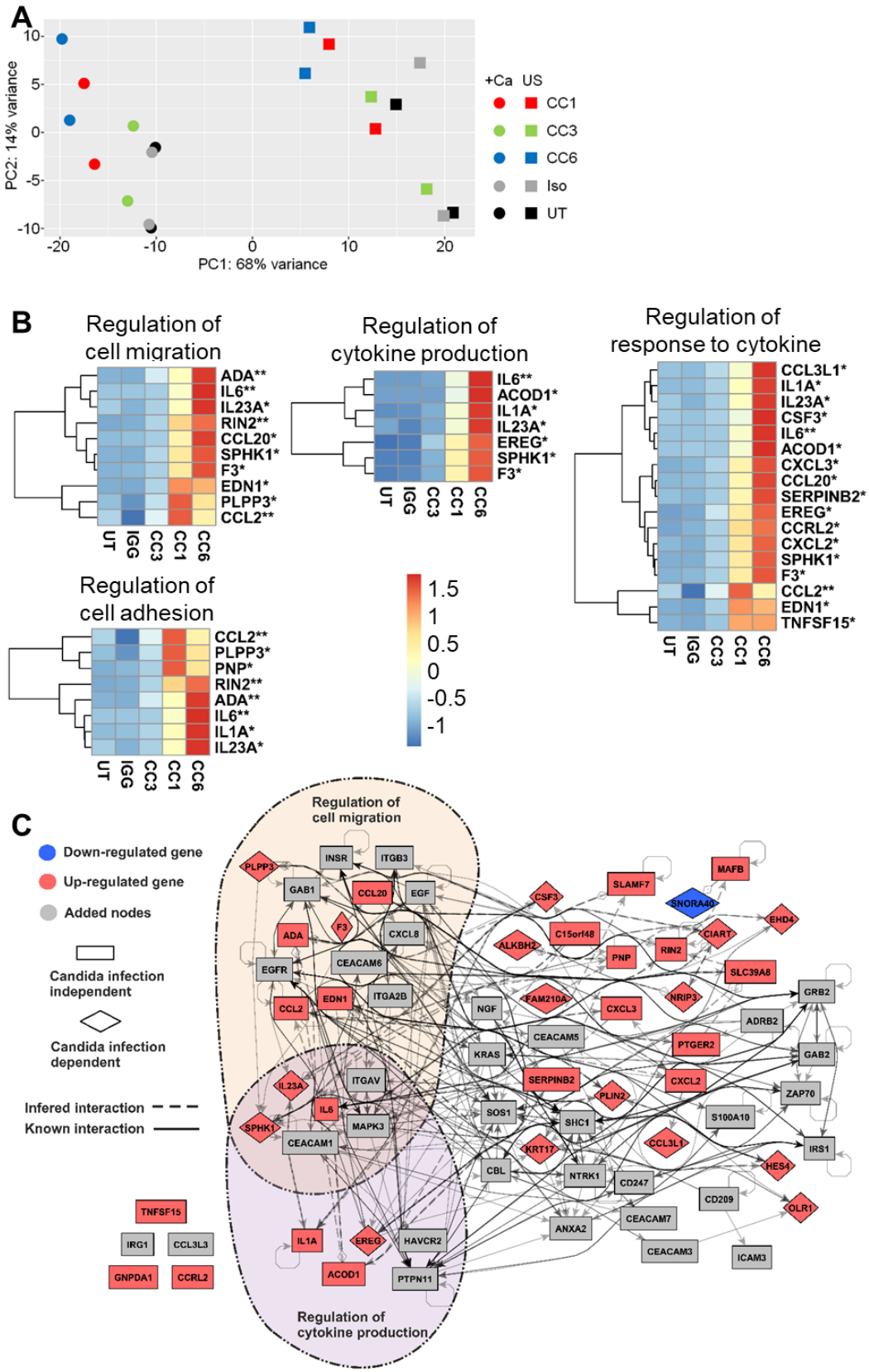

Figure S1: Additional analyses of transcriptomic data. (A) Principal component analysis (PCA) of all samples (untreated, UT; isotype control antibody-treated, Iso; B3-17-treated, CC1, 308/3-3-

treated, CC3; 1H7-4B-treated, CC6) without (US) and with *C. albicans* stimulation (+Ca) presented in Figure 3. (B) Altered *C. albicans*-induced neutrophil transcriptional response after treatment with anti-CEACAM1 antibody. Heat maps display DEGs after CEACAM1 (CC1) treatment in presence of *C. albicans* from major enriched GO categories (adjusted p-value < 0.05 and fold-change >±2; see also Table S1 for a complete list with fold-changes of all DEGs). The relative expression of each gene is shown for all treatment groups with *C. albicans* stimulation (untreated, UT; isotype control antibody-treated, IGG; B3-17-treated, CC1; 308/3-3-treated, CC3; 1H7-4B-treated, CC6). Each row was normalized (mean = 0) and scaled (standard deviation = 1); *also padj < 0.05 for CC6, ** also padj < 0.05 for CC3. Note that "programmed cell death" and "secretion" were not among the enriched GO categories. (C) Signaling network assembled from the DEGs in CC1-treated neutrophils in presence of *C. albicans* stimulation (blue and red nodes, Table S1) and known interactors of CEACAM family receptors (gray nodes). Interactions are inferred from the RNA-seq samples (dashed lines) or obtained from interaction databases (solid lines). Nodes belonging to significantly enriched GO terms important to neutrophil responses are clustered and framed.

Supplemental Figure 2

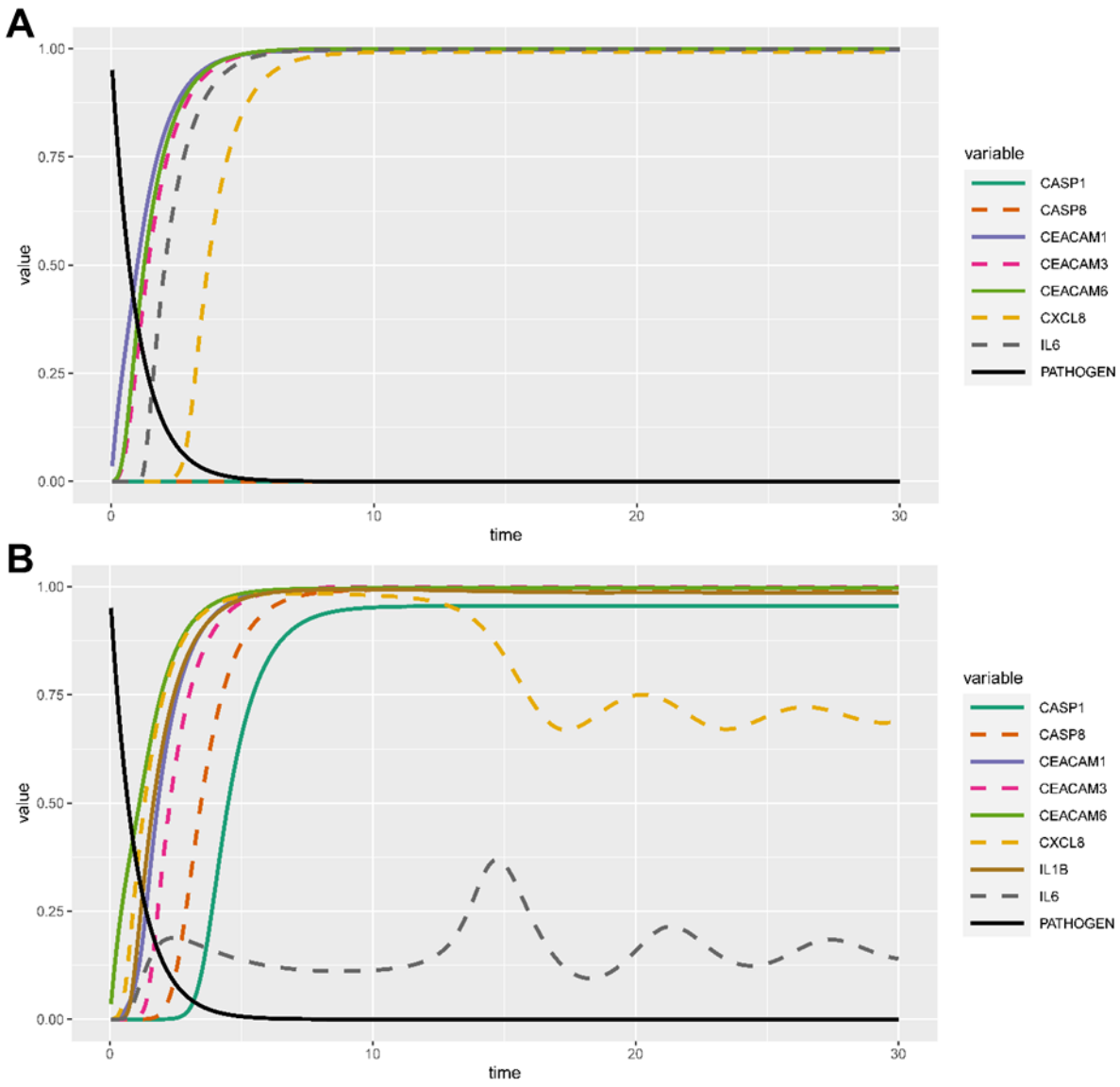

Figure S2. Result curves of the dynamical simulation of Figs. 5 and S1C. The whole networks around the CEACAM receptors and each protein activation pathway was modelled and considered in the dynamical simulation of the pathogen stimulation effects. For the simulations the extra node "PATHOGEN" (for pathogen *C. albicans*) was added to the network; this node is activating and linked to the CEACAM1 (A) and the CEACAM6 (B) node, respectively. The information flow was modeled using Hill functions. Selected trajectories are presented here.